AN INVESTIGATION INTO THE FACTORS AFFECTING PRECOAT PERFORMANCE IN WOVEN-FIBRE MICROFILTRATION

Shadana Vallabh

Submitted in fulfilment of the
academic requirements for the degree of
Master of Technology
Faculty of Engineering
in the
Department of Chemical Engineering
M L Sultan Technikon

February 2002

Declaration

I hereby declare that this dissertation is my own work, unless stated to the contrary in the text, and that it has not been submitted in part, or whole to any other Technikon or Institution. The research was carried out at the M L Sultan Technikon in the Department of Chemical Engineering. The supervisor for the work was Dr. V.L. Pillay.

S Vallabh

February 2002

Acknowledgements

I wish to express my sincere gratitude to the following people, for their contributions towards this dissertation:

(i) Dr Lingam Pillay, the supervisor of the project, for his invaluable input in terms of guidance, assistance, discussions and encouragement.

(ii) Sanjeev Debipersadh and Vischal Rambridge, laboratory assistants of the Department of Chemical Engineering, for constructing the experimental apparatus.

(iii) Mbatha Mduduzi Winston, Sibisi Collen and Mpanza Nkosinomusa Senanelo, members of the Water Technology Group of the Department of Chemical Engineering, for their assistance in conducting the experiments.

(iv) Suresh Ramsuroop, the head of the Department of Chemical Engineering, for his invaluable assistanace, guidance and encouragement.

(v) Members of the Water Technology Group of the Department of Chemical Engineering, for their general assistance.

(vi) My colleagues in the Department of Chemical Engineering and friends for their general encouragement.

(vii) NRF, for sponsoring the project.

Summary

Crossflow microfiltration (CFMF) using a fabric support has been successfully used to treat a range of problematic waters. Experimental evidence indicates that the formation of a dynamic membrane or precoat on a woven-fibre microfilter can significantly increase the performance of the filter, that is, the production rate and rejection. The use of precoats in filtration applications is based on the precoat's unique microstructure that is able to trap sub-micron particles while maintaining a permeable filter cake. However, to date the precoating step has been more of an art than a science. Very little knowledge exists on the best type of precoat to use, or the the optimal velocity, pressure and concentration to form a stable precoat. Further, although various models have been proposed for CFMF, their still exists a lack of knowledge of the mechanisms by which precoats improve performance.

The primary objective of this study was to determine the effect of precoating operating variables (i.e. precoating period, velocity, pressure and concentration) on the performance of the microfilter treating raw surface water, and hence establish an optimal precoating strategy. The secondary objective was to investigate the correlation between average particle size of the precoat and performance of the microfilter. These objectives were accomplished as described below.

A single fabric tube, 25 mm in diameter and 2.3 m long was used as the support. The mode of operation was full recycle i.e. the permeate and reject from the membrane was recombined and reused as the feed suspension. Precoating periods investigated ranged from 15 minutes to 60 minutes, precoating velocities from 1.0 m/s to 3.0 m/s, precoating pressures from 100 kPa to 300 kPa, precoating concentrations from 2 g/l to 50 g/l and average precoat particle sizes from 2 μm to 40 μm. Performance of the precoat was determined by permeate flux and turbidity which was measured throughout. All experiments were performed on precoat slurries of limestone in tap water. The artificial feed suspension which had to have similar fouling properties of raw surface water was

made up using a blend of bentonite and koalin in tap water. The artificial feed suspension was operated at a concentration of 0.05 g/l, a velocity of 1.9 m/s, a pressure of 200 kPa and for a period of 6 hours.

The degree to which the flux is enhanced by the precoat layer was quantified using the parameter Production Ratio. The Production Ratio is obtained by expressing the cumulative volume of permeate obtained using a precoat relative to the cumulative volume of permeate obtained without a precoat. The Production Ratio remains constant after 6 hours of operation hence the steady state Production Ratio was the Production Ratio obtained after 6 hours of operation.

It was found that all of the above-mentioned precoating variables affect the performance of the microfilter. It is observed that the steady state Production Ratio goes through a maximum with an increase in precoat time, velocity and pressure. For precoat concentration and average particle size, the steady state Production Ratio increases at the low concentrations and particle sizes, but the dependence weakens as concentration and particle size reach higher values until finally the steady state Production Ratio reaches a plateau.

The results obtained are not intuitively obvious and suggest that other factors such as hydraulic compression of the cake, the preferential deposition effect and the fines infiltration effect have influenced the specific resistance and hence permeablity of the precoat layer. The optimum precoating conditions obtained in this study using limestone as the precoating material are a precoat time of approximately 30 minutes, a precoat velocity of 2 m/s, a precoat pressure of 200 kPa and an average particle size of 10 microns.

Contents

List of Figures

List of Tables

Nomenclature

c	concentration (g/l)
$J_{precoat,ss}$	quasi steady state flux obtained along the tube length when the feed suspension is filtered through a precoat (l/h.m^2)
$J_{no\ precoat,ss}$	quasi steady state flux obtained along the tube length when the feed suspension is filtered through the membrane only (l/h.m^2)
J(t)	flux obtained along the tube length (l/h.m^2)
$J(t)_{precoat}$	flux obtained along the tube length when the feed suspension is filtered through a precoat (l/h.m^2)
$J(t)_{no\ precoat}$	flux obtained along the tube length when the feed suspension is filtered through the membrane only (l/h.m^2)
l	tube length (m)
P	pressure (kPa)
Q_f	feed flowrate (l/h)
r	tube radius (m)
t	time
t_o	time at the start of the cycle
v	velocity (m/s)
V	volume of permeate produced on a tube length (m^3)

Chapter 1

INTRODUCTION

1.1 BACKGROUND

Crossflow microfiltration (CFMF) is a pressure-driven membrane filtration process used in solid-liquid separation. CFMF is used for concentration of slurries in the food, beverage, cosmetic and biotechnology industries and for the purification and pre-treatment of water. In CFMF the feed suspension is pumped tangentially over the membrane surface. The membrane can be in the form of sheets or tubes. Clear liquid permeates the membrane and is recovered as the permeate. The solids accumulate on the membrane surface forming a cake which decreases the permeate flux. However, the tangential suspension flow scours the cake surface thereby limiting the cake growth. Thus, after an initial rapid decrease, the permeate flux levels off. This is in contrast to the dead-end filtration process in which the cake keeps growing with filtration time.

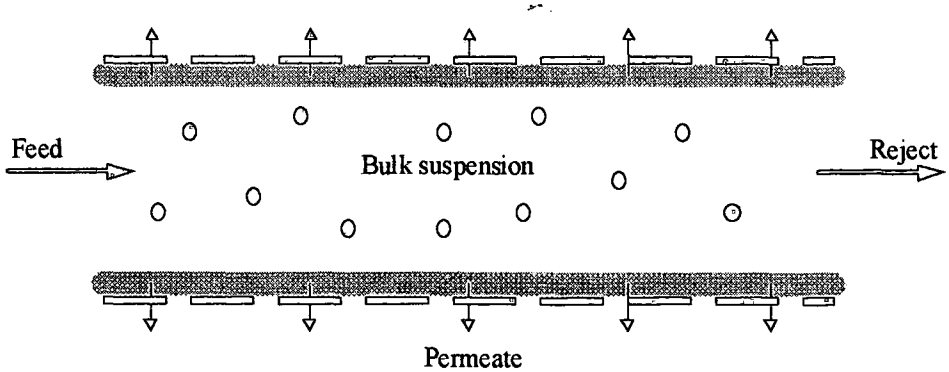

Figure 1.1 Description of CFMF Process

The filtration is carried out by a membrane on a support. This is usually a static, rigid or semi-rigid material. The more common structural materials include sintered metals, porous plastics, ceramics and polymers. The major advantage of these materials is that they maintain their shape and can thus be back-flushed. They also enable operation at high pressure. Although they offer good filtration, they also suffer from a number of disadvantages including difficulty in cleaning, high costs of packaging and installation, and high initial and replacement capital costs.

In comparison membrane supports made from materials such as the woven-fibre tubes can be produced relatively inexpensively in long lengths thus making CFMF more economical for large-scale high-volume applications. In rigid tubes, the tube wall is usually the filtration barrier, and the formation of the cake is undesirable. In woven-fibre tubes the actual filtration barrier is the dynamic cake (or dynamic membrane) that forms on the tube wall. The filtration is usually designed to take place on the dynamic membrane. The purpose of the cloth is to act as a support for the dynamic membrane. The close packing of the dynamic membrane particles can enable the retention of particles that are often orders of magnitude smaller than the pores in the fabric tube wall. This system thus affords the advantage that tubes with relatively large pores may be used, enabling easier cleaning and reducing irreversible fouling of the pores.

The support material can be chemically treated to provide a static membrane which is firmly held in place, or a dynamic membrane which is formed from suspended solids and held on the inside tube wall by the internal operating pressure, or a combination can be used. A dynamic membrane formed from suspended solids other than the suspension to be filtered is, in effect, acting as a precoated membrane filtration system.

The use of precoats in filtration applications is based on the precoat's unique microscopic structure that is able to trap sub-micron particles while maintaining a permeable filter cake. Usually, the use of precoats in microfiltration is a three step operation. First, a layer of the precoat is coated on the membrane surface by recirculating a precoat suspension through the microfilter. This is referred to as 'precoating' the filter. Thereafter, the supension to be treated is filtered and finally the

cleaning of the filter prior to the start of the next cycle. The precoat serves two purposes; it improves the clarity of the filtrate and protects the microfilter from fouling by the fine particles being removed. Thus, higher fluxes are obtained and the production filter cycle is lengthened.

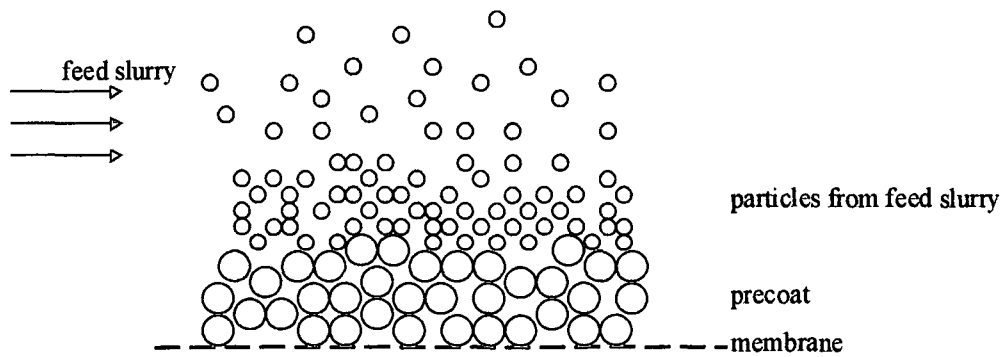

Figure 1.2 Precoat Filtration

Treffry-Goatley et al (1987) used a woven-fibre microfilter to treat a range of problematic waters. A calcium carbonate precoat was used on the tubes to treat raw surface water at a water treatment plant. The microfilter with the calcium carbonate precoat achieved water quality which was comparable to the conventional method of water treatment. The crossflow microfilter was also used to treat a sewage works tertiary effluent using a range of precoats. A seven fold increase in permeate flux and an improved permeate quality was obtained through the selection of the correct precoat layer.

Arora and Davis (1994) performed experiments to study the dead-end microfiltration of bovine serum albumin in the presence of a yeast precoat layer. The permeate flux was appreciably greater with the yeast precoat than without it. Also the yeast precoat greatly reduced the transmission of proteins which would otherwise have fouled the membrane.

The use of precoats on the porous microfiltration membrane reported in the literature [Treffry-Goatley et al (1987) and Arora and Davis (1994)] suggested that the formation of precoats changed the separation ranges of the original support and gave attractive values of permeate flux.

The efficiency of the precoated membrane is expected to be a function of the operating parameters. Most studies reported in the literature lacked the effect of the precoating operating parameters on the performance of the microfilter. To date the precoating step has been an art rather than a science. Very little knowledge exists on the best type of precoat to use, or the optimal velocity, pressure and concentration to form a stable precoat. Further, although various theories have been proposed for the mechanisms by which precoats improve performance, none have been scientifically evaluated.

The scope of the present project is to investigate the effect of the precoat operating variables on the performance of the microfilter processing raw surface water. Microfiltration is becoming increasingly attractive as an alternative to conventional water and waste water treatment. However one of the major obstacles which hinders the application of microfiltration for water and waste water treatment is that the flux declines with time. This phenomenon is commonly termed membrane fouling. Membrane fouling reduces the production rate and increases the complexity of the operation since the system has to be halted frequently to restore the flux by backflushing. The resultant elevated cost makes microfiltration economically less feasible. The application of a precoat prior to filtration of the raw surface water [Treffry-Goatley et al (1987)] has been reported to meet all water quality standards and the process was shown to be advantageous since it eliminates a number of the conventional processing steps. It is, therefore, very interesting to study the potential application of precoats for the purification of raw surface water in which there has been a limited study.

1.2 OBJECTIVES

The specific objectives of the study were as follows:

(i) The effect of precoating variables (i.e. precoating period, velocity, pressure and concentration) on the performance of the microfilter was determined, and hence an optimal precoating strategy established. Performance criteria included permeate flux, turbidity and ease of cleaning.

(ii) The correlation between average particle size of the precoat and performance of the microfilter was investigated.

1.3 APPROACH

A feed suspension which was reproducible and had similar fouling characteristics to raw surface water was determined and a suitable precoat material was chosen.

The feed suspension was filtered without a precoat layer (to construct a base flux-time curve) and then filtered through precoat layers formed under various operating conditions (namely precoat time, velocity, pressure, concentration and average precoat particle size). Each precoating variable was investigated independently.

Permeate flux and time elapsed was measured for each precoating condition. The effect of precoating in filtration was quantified by comparing the flux obtained with a precoat to the flux obtained without a precoat. Production-time curves were drawn for each of the precoating conditions. The trend that the production curves exhibited with respect to precoating time, velocity, pressure, concentration and average particle size was evaluated and a precoating strategy was developed.

1.4 THESIS OUTLINE

The remainder of the dissertation is divided into five chapters.

Chapter 2 deals with the experimental system and procedure. It covers the start-up and operational procedure as well as the basis for choosing the artificial feed suspension to simulate the fouling characteristics of raw surface water. Chapter 3 deals with error estimation and the processing of the experimental results. The degree of flux

enhancement by the precoat layer was quantified by the parameter, Production Ratio, P. The Production Ratio represents the cumulative volume of permeate obtained with a precoat relative to the cumulative volume of permeate obtained without a precoat.

The experimental results are presented in Chapter 4. Chapter 5 first focuses on the formation of the precoat layer and the various mechanisms that contribute to the decline in precoat permeability. This provides some insight as to how the precoat operating variables affect the effectiveness of the precoat layer. The results obtained in the study are then discussed and compared with work done by other researchers.

Chapter 6 concludes the study.

Chapter 2

EXPERIMENTAL SYSTEMS

2.1 APPARATUS

A schematic diagram of the CFMF system used to obtain the experimental results is shown in Figure 2.1.

A single fabric tube 25 mm in diameter and 2.31 m long was used as the support on which the precoat was formed. The apparatus was equipped with a feed tank and a precoating tank, both of 200 litre volume. Both tanks were fitted with stirrers. The tanks were well mixed and no deposition of solids was observed.

Suspension from the tanks were pumped into the CFMF tube by two Hydra-Cell D25 positive displacement pumps driven by a single 7.5 kW ac motor. The positive displacement pump was used to obtain a constant feed flow rate. The pulsating flow normally associated with positive displacement pumps was overcome by the triplex action of the Hydra-Cell pump and an accumulator downstream of the pump. The speed of the motor and hence the flow rate was controlled by a frequency converter. The frequency converter was fitted with a potentiometer in order to set the pumping rate accurately and repeatedly.

The pressure in the tube was controlled by a back-pressure valve at the outlet of the filter hose. A 50 mm rubber lined diaphragm valve was used. Pressure tappings were placed at the entrance to and exit of the CFMF tube. These tappings were connected to a pressure guage. Readings at the entrance and exit could be taken independently via switching valves.

Figure 2.1 Schematic Diagram of Experimental Apparatus

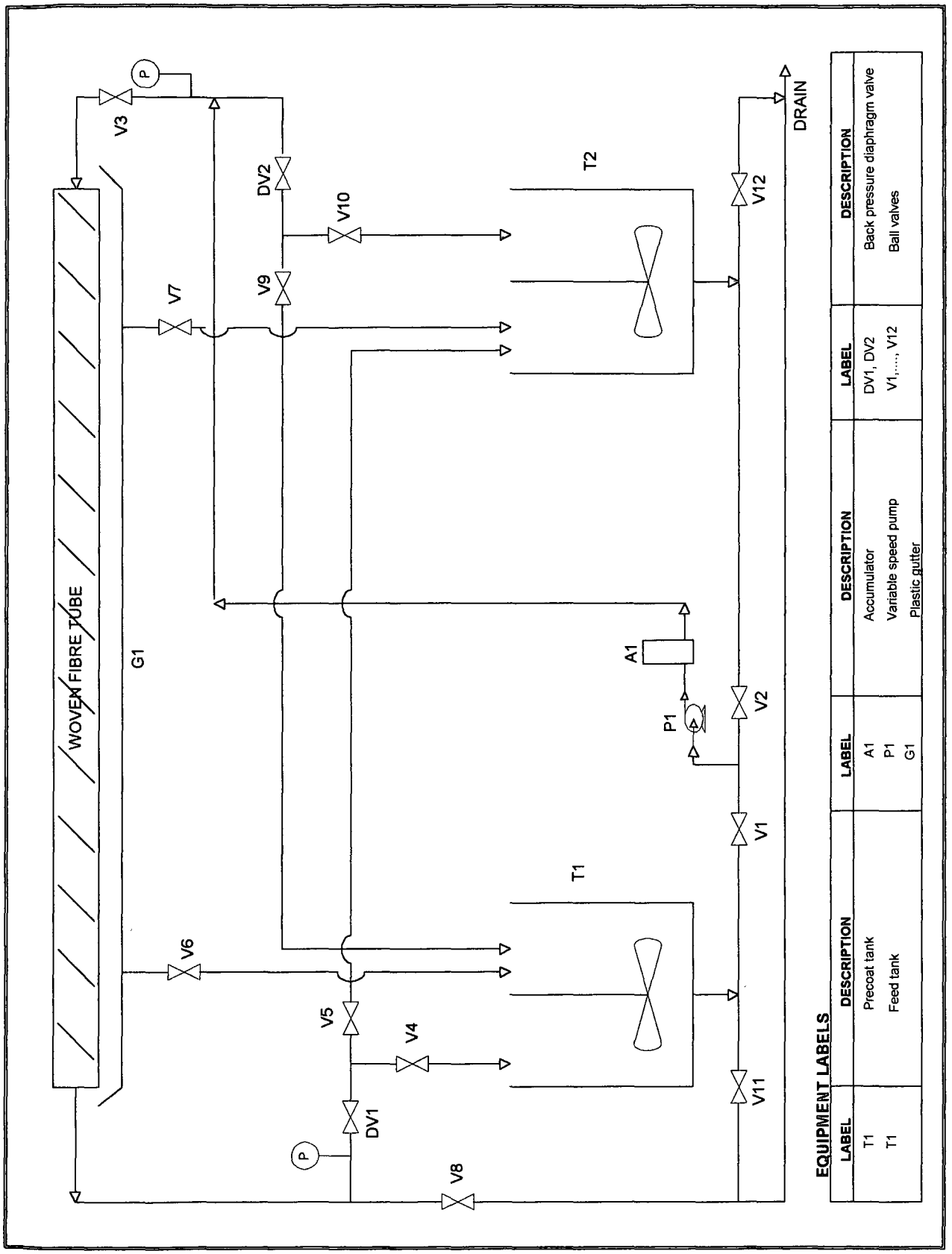

The permeate from the filter tube was collected in a plastic gutter under the tube from where it flowed back into the feed tank. The concentrated slurry was also returned to the feed tank thus the slurry concentration remained constant throughout the duration of an experiment. While the tube was being precoated, the permeate and reject were returned to the precoating tank.

2.2 MEASUREMENT OF PARAMETERS

Temperature

The temperature of the slurry was measured using a mercury thermometer inserted into the slurry tank.

Flux

The permeate flow rate was determined by measuring the time required to collect 1 litre of permeate flowing from the gutter to the feed tank. The flux was calculated by dividing the permeate flow rate by the active tube area. Thereafter the flux was corrected for fluctuations in temperature.

Pressure

The operating pressure was measured at the entrance and exit of the tube using a 0 to 500 kPa glycerine filled pressure gauge.

Concentration

Three samples of the slurry were taken during the experiment in order to determine the slurry concentration. The concentration was measured by drying a measured volume of slurry and measuring the mass of the remaining solids.

2.3 PRECOAT SUSPENSION

A good precoat material should meet four basic requirements. First and the most important, it should be inexpensive. Secondly, it should have a narrow particle size range and a variety of particle shapes for achieving the desired cake permeability. Thirdly, it should be chemically and mechanically stable under operating process conditions. Fourthly, it should be relatively easy to dispose off.

A suspension of pulverised limestone was used as the precoating suspension. It is easily obtainable in several average particle size distributions ranging from d_{50} = 5μm to d_{50} = 40μm and relatively inexpensive. Limestone is generally cubic and forms a permeable precoat. Pillay (1992) used a limestone precoat on a wastewater effluent in order to enhance the flux and rejection and very positive results were obtained in that study.

2.4 ARTIFICIAL FEED SUSPENSION

A dilute artificial suspension which was reproducible and had similar fouling properties to raw surface water was required for this research. The artificial suspension had to have particulates that are typical to the suspended solids in raw surface water and colloidal particles for the highly resistant slimy gel-like layer typical of raw surface water.

Other researchers, who have attempted to characterise surface waters, have done so by adding a commercial clay to distilled water to make up the desired concentration of suspended solids. Some researchers used kaolin while others used bentonite to characterise the fouling properties of surface water in crossflow processes. These suspensions also have about the same size distribution as some of the water components.

Swart (1993) used a blend of bentonite and kaolin in tap water to characterise the fouling properties of surface water in his woven-fibre crossflow microfiltration process. The kaolin represents the suspended solids typical to raw surface water. The bentonite is a type of clay which when mixed with water forms a gel type suspension of high resistance. Swart found that the fouling characteristics of an actual river water suspension and that of a bentonite-kaolin suspension of the same concentration were very similar.

The characterisation of the raw surface water is complex and authors such as Swart have found it difficult to replicate in the laboratory. Since the artificial suspension is not supposed to be a raw surface water standard but a repeatable suspension with similar fouling properties to raw surface water, it was decided to use a blend of bentonite and kaolin. The proportions of bentonite and koalin that would have to be added to water to

simulate the fouling characteristics had to be established. Suspensions of various compositions of bentonite and koalin at different concentrations were made and filtered in the crossflow microfilter. The suspension which had similar filtration behaviour as the raw surface water filtered at the CFMF pilot plant at the Umgeni Water Treatment facility and which had a turbidity in the range of 15 – 30 NTU (nphelometric turbidity unit) was chosen. The suspension chosen for this project was a 1.5 : 1 bentonite : kaolin suspension made up in tap water of concentration 0.05 g/l. The turbidity of the suspension was 18 NTU.

2.5 PROCEDURE

Process operation is in three stages; the application of the precoat to the clean tube, the operation of the process to produce treated water and the cleaning of the tubes prior to the start of the next cycle.

A suspension of pulverised limestone (d_{50} = 50 um), was used as the precoating suspension. The limestone suspension and the bentonite-koalin feed suspension was made up in the precoating tank and feed tank respectively, to the desired concentration. The flow rate was then set to the desired value by adjusting the speed of the pump via the frequency invertor. The system was started up and the limestone suspension flowed into the CFMF tube. The operating flow rate was generally achieved within 20 seconds. The downstream pressure was then increased rapidly up to the desired operating pressure by closing the downstream back pressure valve. Initially the pressure tended to increase and had to be continually adjusted to the operation point by adjusting the back pressure valve. After about 5 minutes the system settled and only occasional adjustments to the back pressure valve were necessary.

After the precoating cycle, the flow to the pump suction was switched from the precoating to the bentonite-koalin feed suspension. Valve V2 was then opened and valve V1 closed. The return line was purged to the precoat tank for a short while to prevent any residual precoating material from entering the feed tank. The feed suspension for all experiments was circulated at 0.05 g/l, 2 m/s and 200 kPa for a period

of 6 hours. In all experiments reported here the permeate was clear to the eye from start up.

The cleaning of the filter tube was achieved by a pulsating flow of water through the tube. This dislodged the solids and conveyed it out of the tube. The total cleaning time was 15 to 20 minutes.

Chapter 3

DATA PROCESSING AND ERROR ANALYSIS

3.1 PRIMARY MEASUREMENTS

Table 3.1 lists the various measurements that were taken, the range of values and estimated maximum and minimum errors associated with each variable.

Table 3.1 : Values and Uncertainties in Primary Measurements

	Value	Uncertainty	% Uncertainty
Equipment variables			
Tube radius (m)	0.0127	0.00025	1.97
Tube length (m)	2.31	0.005	0.22
Operating variables			
Flowrate (l/h)	1800 to 5500	50	0.91 to 2.78
Pressure (kPa)	100 to 300	3	1.0 to 3.0
Precoat concentration (g/l)	2 to 50	0.3	0.60 to 15.0
Feed concentration (g/l)	0.05	0.0003	0.6
Measured variables			
Volume of permeate collected (l)	1	0.01	1.0
Time to collect permeate (s)	10 to 90	0.4	0.44 to 4.0
Turbidity feed (NTU)	18	1	5.56
Turbidity permeate (NTU)	0.05 to 9		

3.2 CALCULATION OF PERMEATE FLUX AND SUPERFICIAL INLET VELOCITY

3.2.1 Permeate Flux

$$\text{Permeate Flux } (\ell/\text{m}^2.\text{h}) = \frac{\text{Permeate Flowrate}}{\text{Filtration Area}} \times \frac{3600}{1}$$

$$= \frac{V}{t} \times \frac{1}{2\pi r\ell} \times \frac{3600}{1}$$

$$= \frac{V}{t} \times \frac{1}{0.0252\pi\ell} \times \frac{3600}{1}$$

3.2.2 Superficial Inlet Velocity

$$\text{Superficial Inlet Velocity (m/s)} = \frac{\text{Feed Flowrate}}{\text{Flow Area}} \times \frac{1}{3600} \times \frac{1}{1000}$$

$$= \frac{Q_f}{\pi r^2} \times \frac{1}{3\,600\,000}$$

$$= \frac{Q_f}{\pi.(0.0126)^2} \times \frac{1}{3\,600\,000}$$

$$= \frac{Q_f}{1795.5}$$

3.3 ERROR ANALYSIS

The percentage uncertainty associated with each of the calculations in Sec 3.2 is given by the largest percentage uncertainty among the independent variables given in Table 3.1.

3.3.1 Uncertainty in Permeate Flux

Variable	Uncertainty
Permeate flowrate	1 %
Time	4 %
Diameter	1.97 %
Length	0.22 %
Maximum uncertainty	**2 %**

3.3.2 Uncertainty in Superficial Inlet Velocity

Variable	Uncertainty
Feed flowrate	2.78
Diameter	2 x 1.97
Maximum uncertainty	**4%**

3.3.3 Errors in Flux-Time Curves

There are two sources of errors inherent in the flux-time curves reported in Chapter 4:

(i) Uncertainty in the flux value, 4 %.

(ii) Uncertainty in the time at which the flux is plotted. Assume t_{perm} is the time taken to measure a quantity of permeate and t is the time at which the measuring began. The flux has been plotted at time t, rather than the mean time of $t + \frac{1}{2}t_{perm}$.

A typical flux-time curve, with an uncertainty envelope, is shown in Figure 3.1. It can be seen that the uncertainties are clearly insignificant and have not been included in subsequent flux-time curves.

Figure 3.1 : A graph showing the uncertainty associated with a typical CFMF flux-time curve. The artificial feed suspension was operated at a concentration of 0.05 g/l, a velocity of 1.9 m/s and a pressure of 200 kPa.

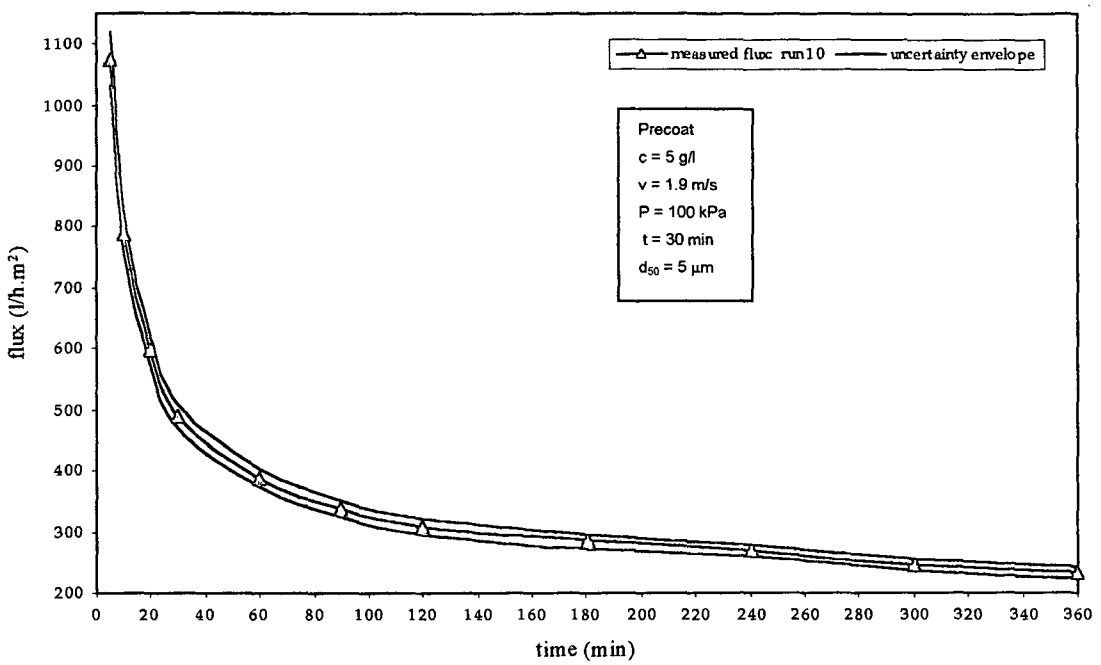

3.3.4 Repeatability

Several experiments were conducted at similar operating conditions in order to establish the repeatability of the experiments. Figure 3.2 and Figure 3.3 show experiments for the precoat flux and the feed suspension flux respectively, conducted under similar operating conditions. For both the precoat and feed suspension, repeatability is good.

Figure 3.2 : A graph showing flux-time curves for the precoat suspension for different experiments conducted under similar operating conditions in order to establish the repeatability of the experiments.

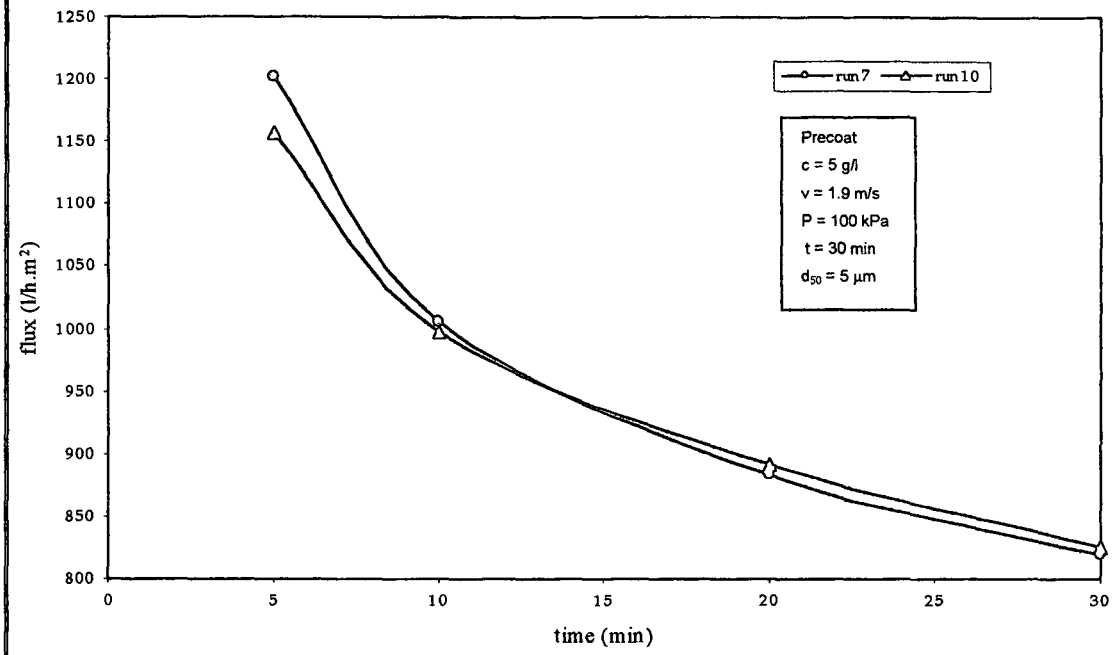

Figure 3.3 : A graph showing flux-time curves for the artificial feed suspension for different experiments conducted under similar operating conditions in order to establish the repeatability of the experiments.

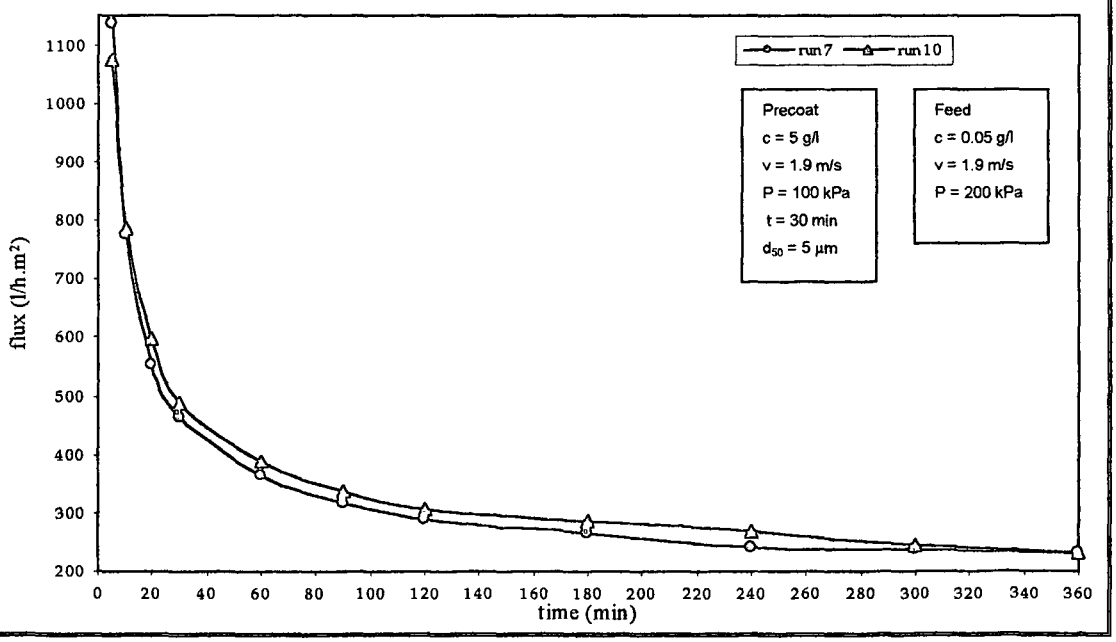

3.4 PROCESSING OF EXPERIMENTAL RESULTS

The manner in which the experimental results were processed and the parameter used to quantify the degree of flux enhancement by the precoat layer will be outlined.

3.4.1 Introduction

A typical flux enhancement by the precoat layer is shown by the flux-time curves presented in Figure 3.4. The curve for run 1 represents the flux obtained when the artificial feed suspension was filtered without a layer of precoat. The curve for run 5 represents the flux obtained when the artificial feed suspension was filtered through a precoat layer. The precoat layer was formed when a precoat suspension which had a concentration of 5 g/l and an average particle size of 5 microns, was filtered for 30 minutes at 2.5 m/s and 200 kPa prior to the artificial feed suspension. It should also be noted that time zero minutes is taken at the start of the switchover from the precoat suspension to the feed suspension.

Figure 3.4 : Graph showing a comparison between the flux profiles of unprecoated and precoated experiments.

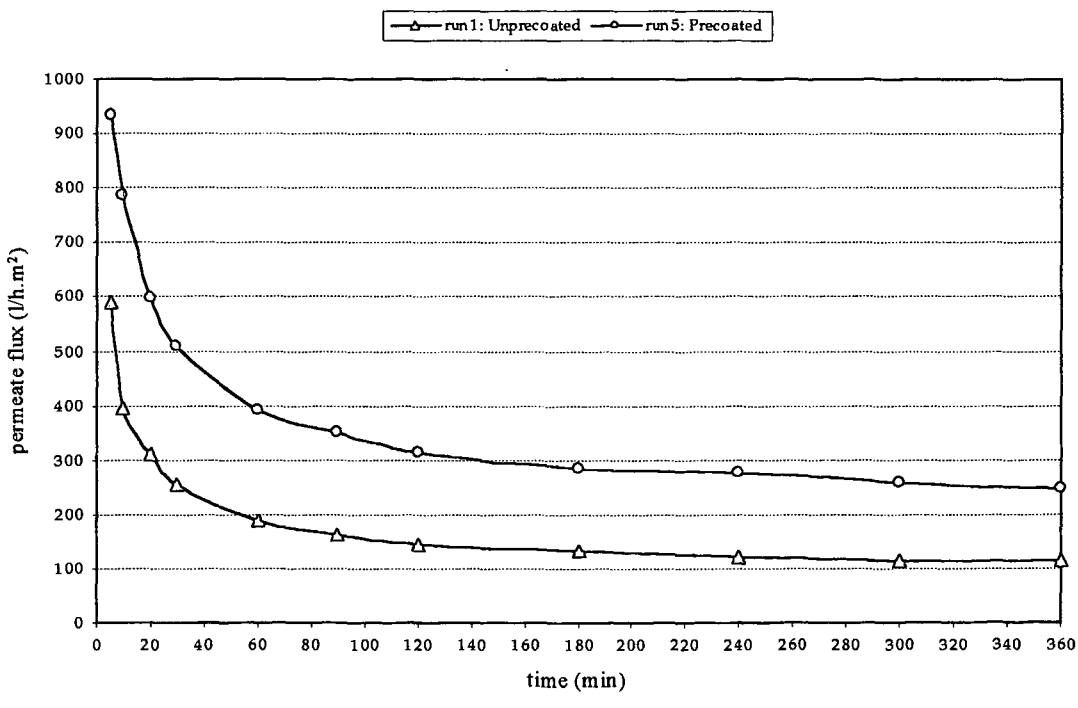

During crossflow microfiltration, particles are dragged toward the membrane surface to form a cake. The permeate flux decays continuously as the thickness of the cake is increased, until a quasi-steady state is reached. Ideally the thickness of the cake and the permeate flux remain unchanged after reaching a quasi steady state. However, a typical relationship between the permeate flux and filtration time in this study is shown in Figure 3.5.

Figure 3.5 : Typical Flux-Time Curve

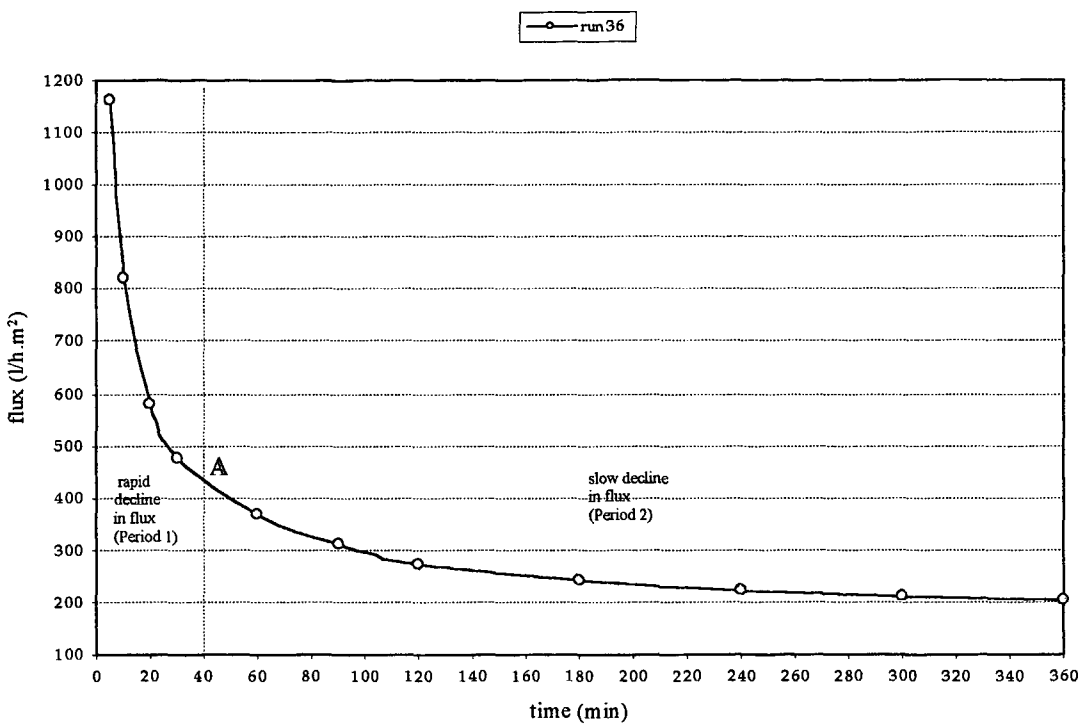

This figure shows that the filtration curve may be divided into two periods. In period 1, the flux decreases rapidly, whereas the flux decays slowly with time in period 2. Note that in this figure that a true steady state is not reached even for a filtration time of 6 hours. Similar behaviour was observed by Swart (1993) and Pillay (1992) in the filtration of suspensions of mixed size particles. Pillay pointed out that the initial rapid decrease in flux is caused by an initial rapid increase in cake thickness. Thereafter the cake thickness remains relatively constant, but the cake is progressively infiltrated by

finer particles resulting in a slow decrease in permeability, and hence the slow long term decline in flux. Baker et al (1985) also reached similar conclusions in their crossflow study of mineral suspensions. Lee and Clark (1998) pointed out that a true steady state permeate flux will be established when there is no more particle accumulation in the cake layer. At this point, the particle deposition rate is in equilibrium with the particle removal rate.

Although the permeate flux does not reach a time independent value, most researchers [Pillay (1992), Wakeman (1994), Hwang et al (1996) to name a few] define the permeate flux at the start point A of period 2 as the quasi steady state permeate flux or the psuedo steady state permeate flux. That is the boundary between the periods is taken as the point where the flux first starts exhibiting the linear decrease with time.

3.4.2 Quantifying Performance using Quasi Steady State Flux

In this study the degree to which the permeate flux is enhanced by the precoat layer needs to be quantified. One way to do this is to compare the quasi steady state flux obtained using a precoat to the flux obtained without a precoat.

$$\text{Performance} = \frac{J_{precoat,ss}}{J_{no\ precoat,ss}}$$

where $J_{precoat,ss}$ is the quasi steady state flux obtained along the tube length when the artificial feed suspension is filtered through a precoat layer

$J_{no\ precoat,ss}$ is the quasi steady state flux obtained along the tube length when the artificial feed suspension is filtered through the membrane only

Where exactly one decides is the boundary between period 1 and period 2 is clearly quite arbitrary. So instead of plotting the Performance ratio for selected times after the quasi steady state was reached, it was decided to plot the Performance ratio for various filtration times covering the entire span of filtration. This would give an indication of what the Performance curve looks like at the start of filtration as compared to what it is

once quasi steady state has been reached. The Performance curve obtained for experimental run 5 is as illustrated in Figure 3.6.

Figure 3.6 : Graph showing the Performance curve obtained for experimental run 5. The precoat suspension had a concentration of 5 g/l, velocity of 2.5 m/s, pressure of 200 kPa, precoat time of 30 minutes and a d_{50} of 5 microns.

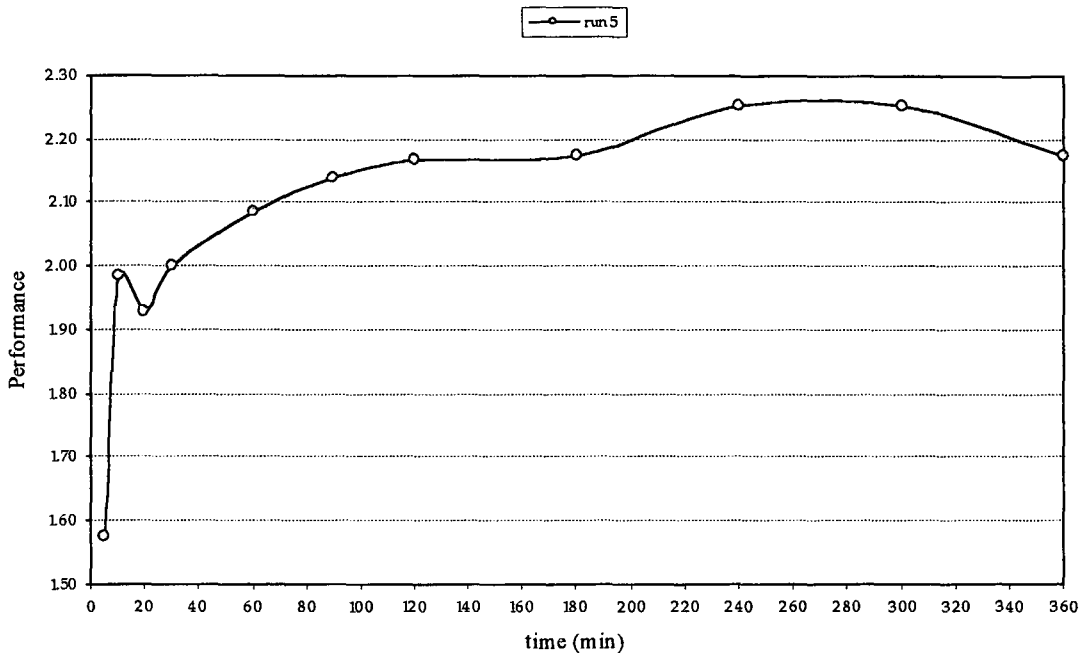

Initially there is a rapid increase in the Performance up until approximately 40 minutes. Thereafter there is a general slow increase in the Performance. It does not remain constant as was expected. After 40 minutes the Performance varies between 2.0 and 2.3, that is the permeate flux obtained when the artificial feed suspension is filtered with a precoat could be enhanced at least two-fold or a maximum of 2.3 times as compared to when the artificial feed suspension is filtered without a precoat. A similar trend was observed when the Performance curves were drawn for when the artificial feed suspension is filtered through precoats formed at various velocities. These curves are presented in Figure 3.7.

Figure 3.7 : Figure showing a family of velocity Performance curves obtained if the entire duration of the experiment is considered.

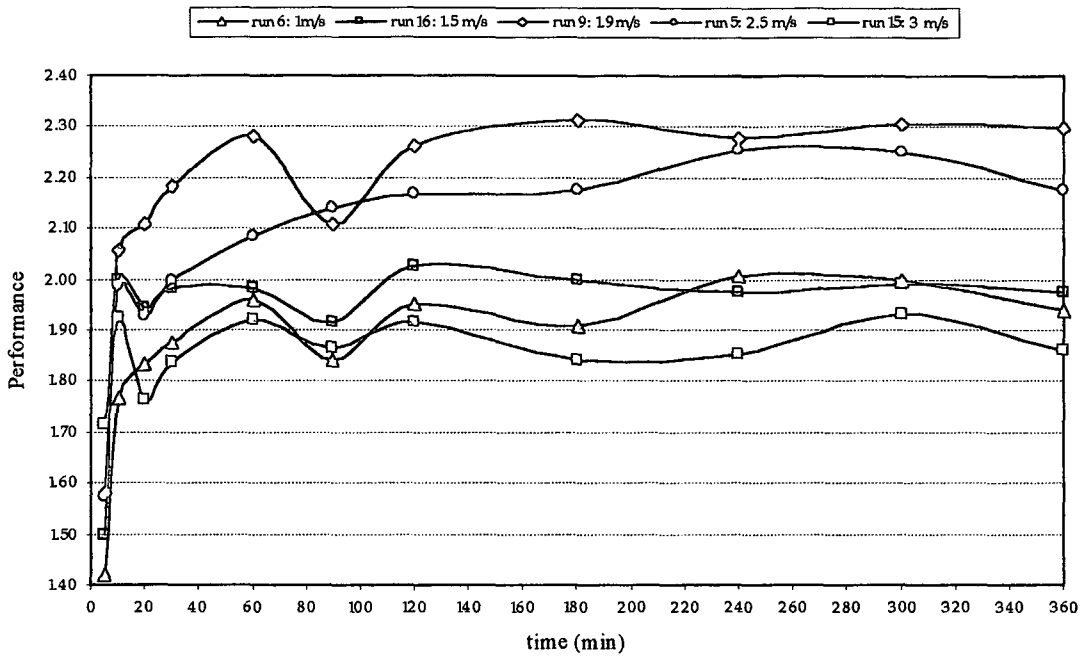

From Figure 3.7 it can be seen that the Performance does not remain constant once quasi steady state is reached hence making it difficult to say what the exact Performance is. Due to the steady decline of permeate flux and no true steady state being reached, one does not obtain a constant Performance, which makes it an unsuitable method of quantifying the flux enhancement by the precoat layer.

3.4.3 Concept of Production Ratio

Clearly an alternate method of comparison needs to be developed. From the literature that was surveyed, no method to quantify the flux enhancement by the precoat layer could be found. However, from a practical viewpoint, the net production of filtrate is important, that is the cumulative volume of filtrate obtained. It was then decided to compare the cumulative volume curve obtained when the artificial feed suspension was filtered with a precoat layer as to that when the artificial feed suspension was filtered without a precoat layer. Figure 3.8 illustrates the curves obtained.

Figure 3.8 : Graph showing the cumulative volume of permeate produced vs time for the unprecoated and precoated experiments.

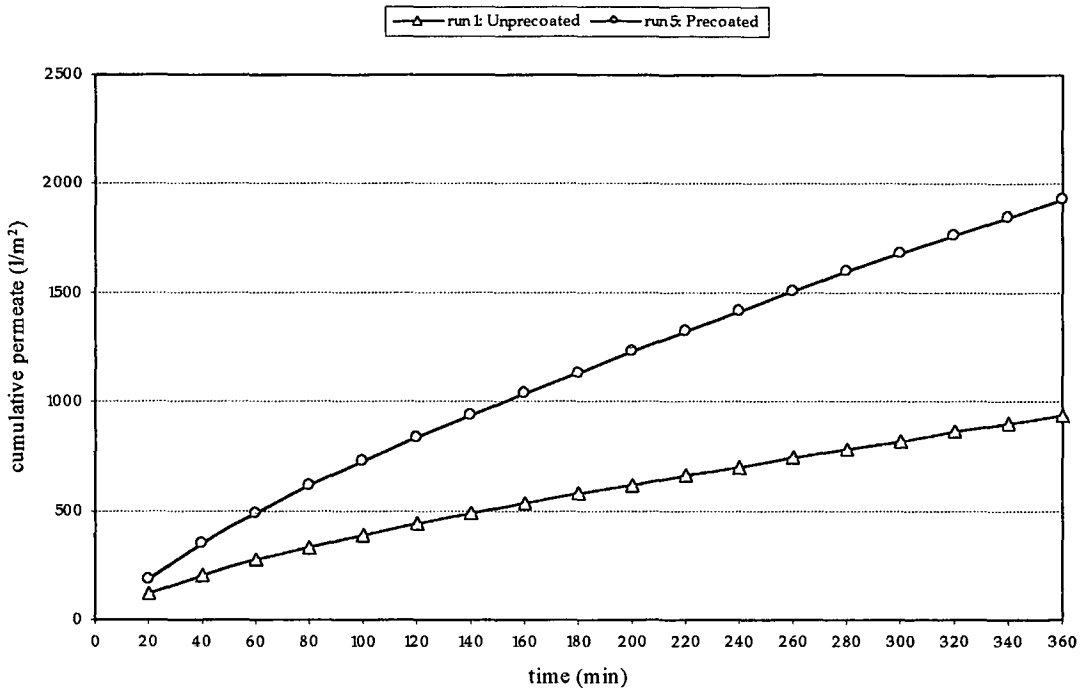

The cumulative volume is obtained as follows:

$$\text{cumulative volume} = \int_{t_o}^{t} J(t)\, dt$$

where J(t) is the permeate flux obtained along the tube length

t_o is the initial time of filtration

t is the final time of filtration

The curves in Figure 3.8 were plotted by integrating the flux shown in Figure 3.4. It should be noted that the cumulative volume from time t = 40 minutes to time t = 60 minutes was plotted at a time of t = 60 minutes. Similarly the cumulative volume from t = 40 minutes to t = 80 minutes was plotted at a time of t = 80 minutes and so forth.

From Figure 3.8 it seems that after 100 minutes the curves are essentially linear. Therefore the ratio of cumulative volume obtained when filtering through a precoat layer to the cumulative volume obtained when filtering without a precoat layer should

be fairly constant. It was then decided to plot this ratio to see if it did in fact come out to be fairly constant. This ratio was expressed using a parameter Production Ratio.

$$\text{Production Ratio} = \frac{\text{cumulative volume obtained when filtering using a precoat}}{\text{cumulative volume obtained when filtering without a precoat}}$$

$$\text{Production Ratio} = \frac{\int_{t_o}^{t} J(t)_{precoat}\, dt}{\int_{t_o}^{t} J(t)_{no\ precoat}\, dt}$$

The Production Ratio quantifies the increase in flux by the precoat layer in terms of permeate produced per square meter. This ratio was plotted for the curves shown in Figure 3.8 and the Production curve obtained is as illustrated in Figure 3.9.

Figure 3.9 : Graph showing the Production Ratio curve obtained for experimental run 5. The precoat suspension had a concentration of 5 g/l, velocity of 2.5 m/s, pressure of 200 kPa, precoat time of 30 minutes and a d_{50} of 5 microns.

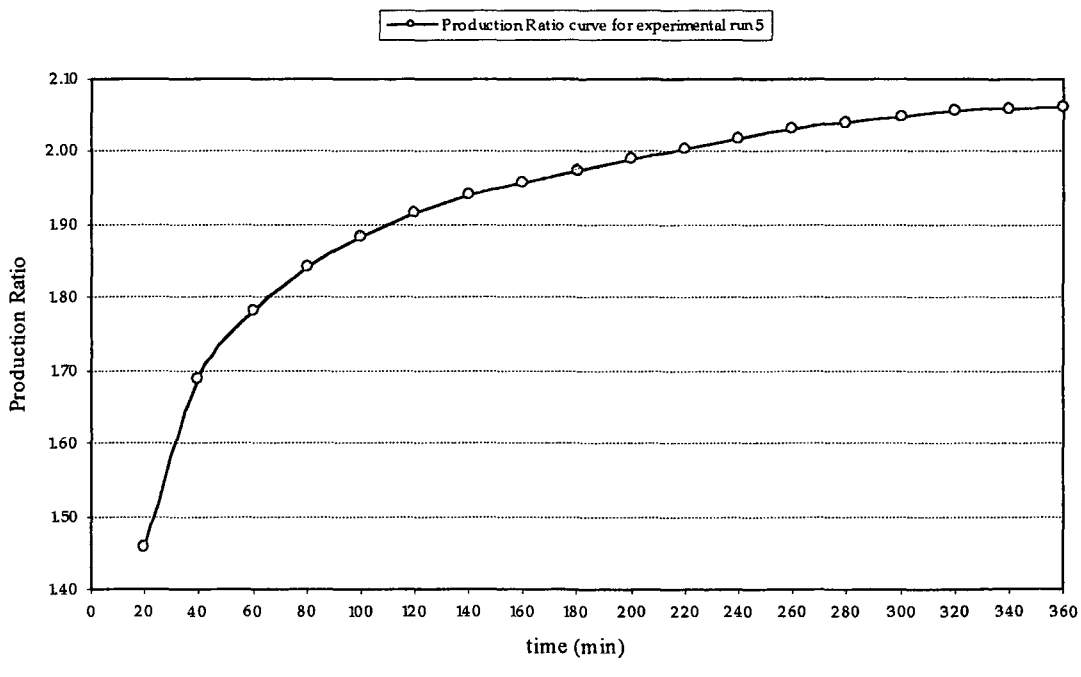

Initially the Production Ratio increases rapidly and then starts asymtoting. It was thought that the initial rapid decrease in flux during the first 40 minutes would affect the Production Ratio. Due to the flux being very high during the initial period, it is not possible to obtain accurate flux measurements. If the first 40 minutes of the flux-time curve is ignored the Production Ratio curve obtained is as illustrated in Figure 3.10.

Figure 3.10 : Graph showing the comparison of the Production Ratio curve obtained if the entire duration of the experiment is considered and the Production Ratio curve obtained if the first 40 minutes of the experiment is ignored.

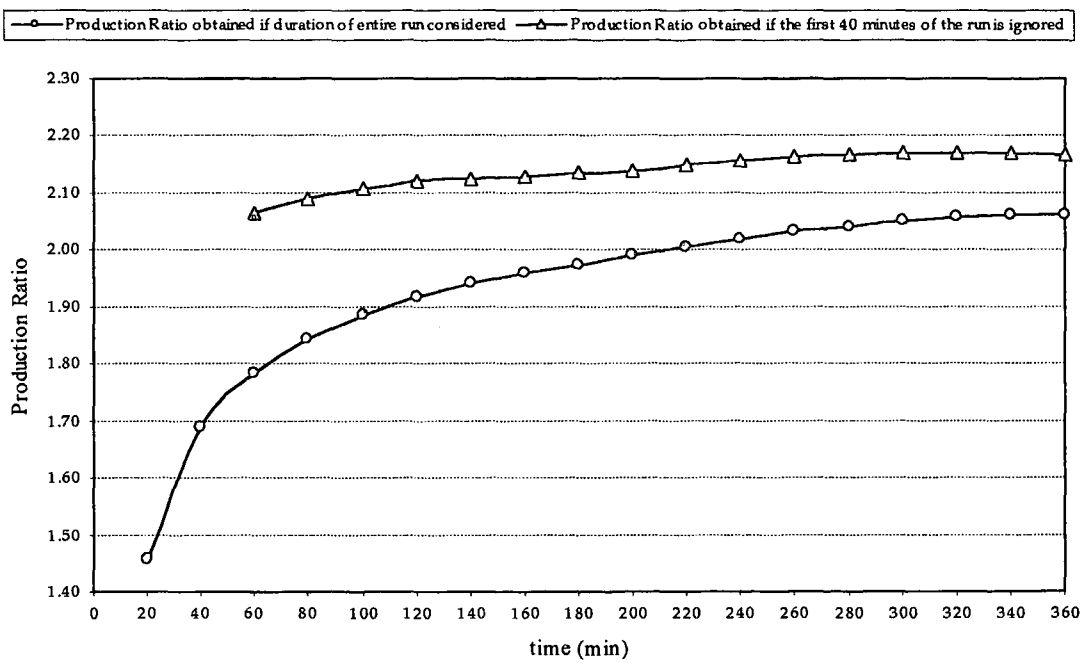

From Figure 3.10, one can see that the Production curve moves up slightly from approximately 2.05 to 2.17, but remains constant after 4 hours. The upward shift in the curve quantifies an increase in Production Ratio of approximately 5.5%. This implies that the system is not significantly affected if the first 40 minutes of operation is ignored.

So far for the set of results presented, the Production Ratio seems to be a good performance indicator. In order to determine whether the Production Ratio is really an

effective indicator of performance a family of curves was considered. Again a family of Production Ratio curves obtained at different velocities is considered as illustrated in Figure 3.11. The trend observed is similar to the initial Production Ratio curve presented in Figure 3.9. There appears to be a definite trend, that is initially the Production Ratio rapidly increases and thereafter remains relatively constant. However it should be noted that after 360 minutes there is still an increase, albeit very slightly.

Figure 3.11 : Figure showing a family of Production Ratio curves obtained at different precoat velocities.

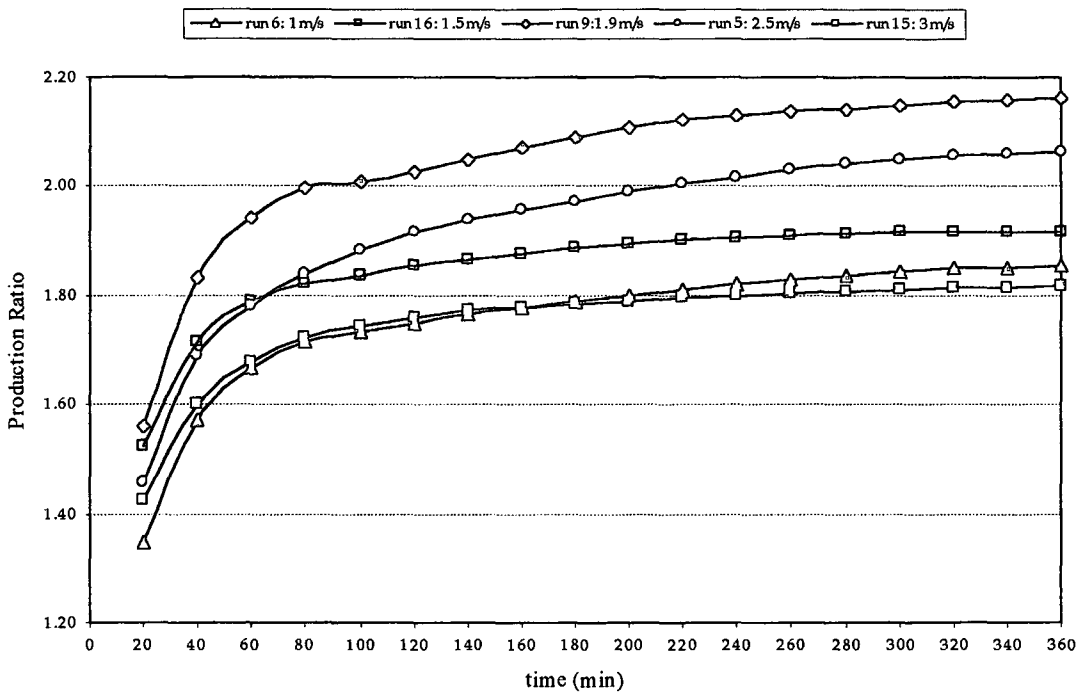

For the Production curves obtained in Figure 3.11, the initial 40 minutes of rapid flux decline was ignored for comparison. The resulting Production Curves obtained are presented in Figure 3.12.

Figure 3.12 : Figure showing the comparison of a family of Production Ratio curves obtained at different precoat velocities and if the first 40 minutes of the experiment is ignored.

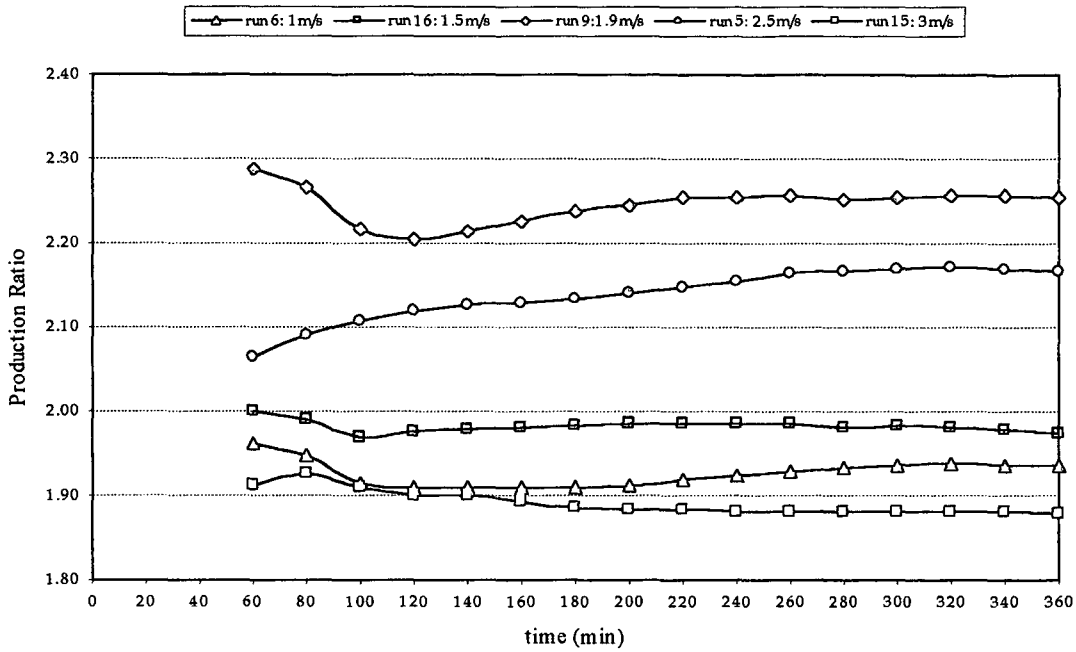

Again an upward shift in all the curves is observed. There is an average increase in Production Ratio of approximately 3.8%. Clearly whether one chooses to ignore the initial period of rapid flux decline or not would not affect the final analysis of the system, as all the curves would be offset by a percentage of approximately 3.8%. Seeing that the increase in Production Ratio with this is insignificant, it was decided to consider the entire duration of filter operation.

From all the experimental results obtained, it was observed that after 4 hours of filter operation, the Production Ratio remained constant, thus making it an effective indicator of performance.

Henceforth it was decided to use the Production Ratio to quantify the flux enhancement by the precoat layer. Seeing that the Production Ratio remains constant after 4 hours of filter operation, the Production Ratio obtained at the end of the 6 hours of filter

operation will be regarded as the steady state Production Ratio if the filter is operated for periods longer than that.

3.4.4 Summary

The performance of the microfilter with a precoat layer had to be quantified. In all experiments, the flux initially decreases rapidly and thereafter declines slowly with time. A true steady state flux is not attained even for a filtration time of 6 hours. Due to the continued decline in flux, the flux was found to be unsuitable to express the degree to which the performance of the microfilter is enhanced by the precoat layer.

From the literature that was surveyed, no method to quantify the flux enhancement by the precoat layer could be found. However, from a practical viewpoint, the net production of filtrate is important, that is the cumulative volume of filtrate obtained. From the plots of cumulative volume of permeate produced it seemed that the ratio of cumulative volume obtained using a precoat layer to the cumulative volume obtained without a precoat layer is constant after 100 minutes. This ratio was expressed using a parameter Production Ratio.

The Production Ratio initially increases rapidly and thereafter levels off. The ratio remains essentially constant after 4 hours of operation. This trend was true for a family of curves and later for all experiments. So it could be said with certainty that the ratio obtained after 6 hours of operation (the duration of all experiments) will be the steady state Production Ratio if the microfilter is to be operated for periods longer than that.

Hence the performance of the microfilter with a precoat layer was quantified using the Production Ratio. The Production Ratio quantifies the increase in flux by the precoat layer in terms of permeate produced per square meter.

Chapter 4

RESULTS

4.1 EXPERIMENTAL METHODOLOGY

Experiments covered the influence of precoating operating variables namely precoat time, velocity, pressure, concentration and particle size. Each variable was investigated independently. Permeate flux and elapsed time were measured throughout.

Economic velocities for CFMF are generally considered to lie between 1 and 3 m/s. Five velocities were chosen namely 1.0 ; 1.5 ; 1.9 ; 2.5 and 3.0 m/s. When the velocity was not being varied, the precoat suspension was operated at 1.9 m/s.

The woven-fibre crossflow filter can withstand pressures up to 400 kPa. The system was run at five different pressures namely 100 ; 150 ; 200 ; 250 and 300 kPa. A pressure of 200 kPa was chosen when the pressure was held constant.

Precoating times of 15 ; 20 ; 25 ; 30 ; 40 and 60 min were chosen. When the precoating period was not being varied, the precoat was operated for a period of 30 minutes. It was found that the permeate flux remained fairly constant after 25-30 minutes (see Figure 5.6, Section 5.5).

Five precoat concentrations were chosen at approximately 2 ; 5 ; 10 ; 20 and 50 g/l. A precoat concentration of 5 g/l was chosen when the concentration was not the variable being investigated. A concentration in the lower range of the span was chosen as too high a concentration would render the use of a precoat expensive.

The precoat material, limestone, was available in four different particle sizes. Experiments covering the effect of particle size on performance of the filter was done using limestone having an average particle size of 2 ; 5 ; 10 and 40 μm. Limestone having a particle size of 5 μm was used when the particle size was held constant.

The artificial suspension was operated for a period of 6 hours at a concentration of 0.05 g/l, a velocity of 1.9 m/s and a pressure of 200 kPa for all experiments.

An experimental matrix is shown in Table 4.1. The experiments were performed in random order and the point (30 minutes, 1.9 m/s, 200 kPa, 5 g/l and average particle size of 5 μm) was used as the reference point. The reference point was repeated after several experiments were completed. The entire matrix was completed as well as additional experiments spanning further points in the ranges considered, in order to verify the trends being obtained.

Table 4.1 : **A matrix showing the experimental design for the CFMF experiments. The experiment numbers are shown on the matrix and coincide with the order in which the experiments were performed.**

Precoat Time (min)	**15**	**20**	**25**	**30**	**40**	**60**
	24, 26	19, 21	23, 25	9	38, 40	18, 20
Velocity (m/s)	**1**	**1.5**	**1.9**	**2.5**	**3**	
	3, 6	16	2, 9, 31, 32, 39, 43	4, 5	15, 42	
Pressure (kPa)	**100**	**150**	**200**	**250**	**300**	
	7, 10	13	9	14	8, 41	
Concentration (g/l)	**2**	**5**	**10**	**20**	**50**	
	11	9	17, 33	12, 34		
Average Particle size (μm)	**2**	**5**	**10**	**40**		
	27, 35	9	28, 30	29, 36		

4.2 EXPERIMENTAL RESULTS

Experiments covered the influence of the precoat operating variables: precoat time,velocity, pressure, concentration and average particle size. The experimental results obtained will be presented.

4.2.1 Permeate Quality

The permeate quality or turbidity was monitored in approximately fifty percent of the CFMF experiments. Turbidity was not monitored for all experiments due to the turbidity meter not being available for use throughout this study. A typical turbidity profile is shown in Figure 4.1.

It was found that in most experiments, a permeate turbidity of below 0.5 NTU was achieved within 60 minutes of start-up. In some experiments the turbidities were high in comparison to theothers. This was attributed to the permeate gutter not being properly cleaned prior to start-up. During the course of this study a very tiny pinhole developed in the very front-end of the membrane filter. Hence a residue of limestone accumulated in the corner of the permeate gutter after several experiments. A typical turbidity profile is shown in Figure 4.1.

Figure 4.1 : A typical permeate turbidity profile.

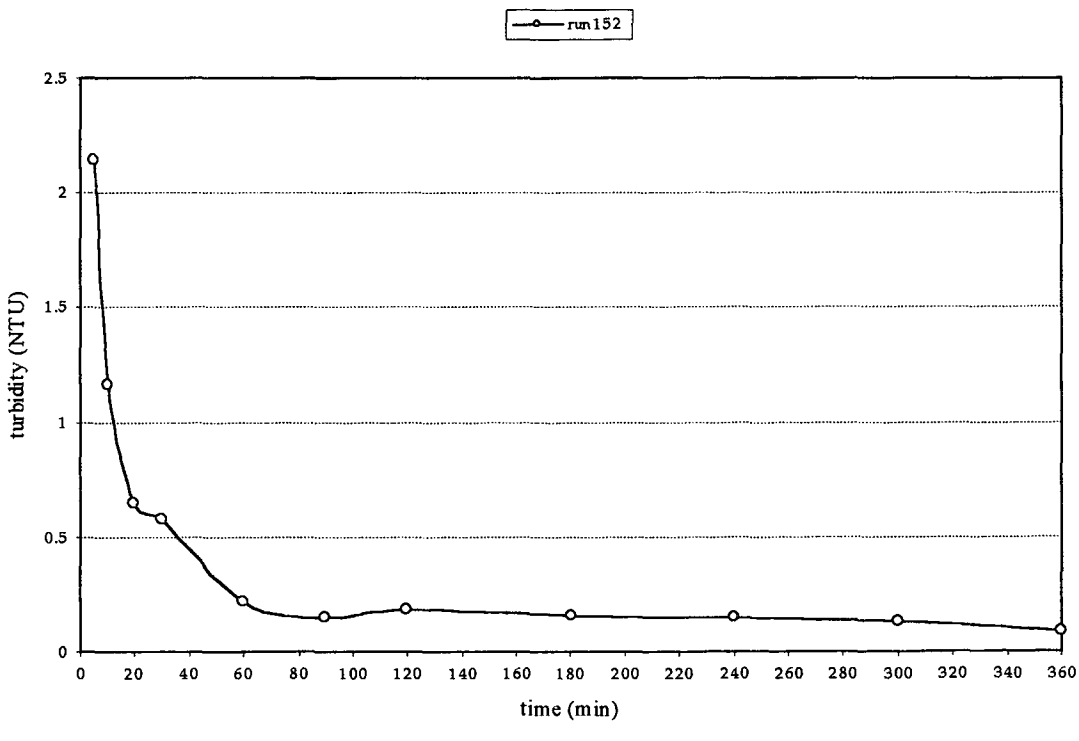

4.2.2 Effect of Precoat Time

For all experiments the precoat velocity, pressure, concentration and average particle size were maintained constant with only the precoating period varying. The effect of precoating time on the permeate flux is illustrated in Figure 4.2(a). It appears as if precoat time has no significant effect on the permeate flux. However, if Figure 4.2(a) is expanded as shown in Figure 4.2(b), the variation in permeate flux is noticeable.

Figure 4.2(a) : Figure showing the effect of the variation of precoat time on flux at a precoat concentration of 5 g/l, a velocity of 1.9 m/s, a pressure of 200 kPa and a d_{50} of 5 microns.

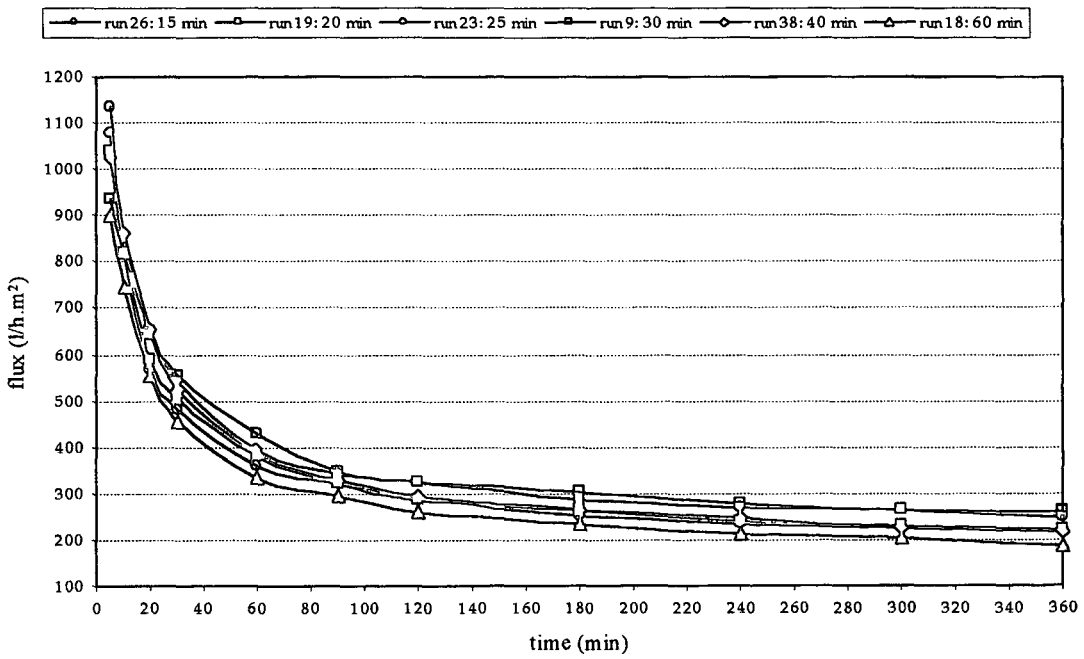

Figure 4.2(b) : Figure 4.2(a) expanded

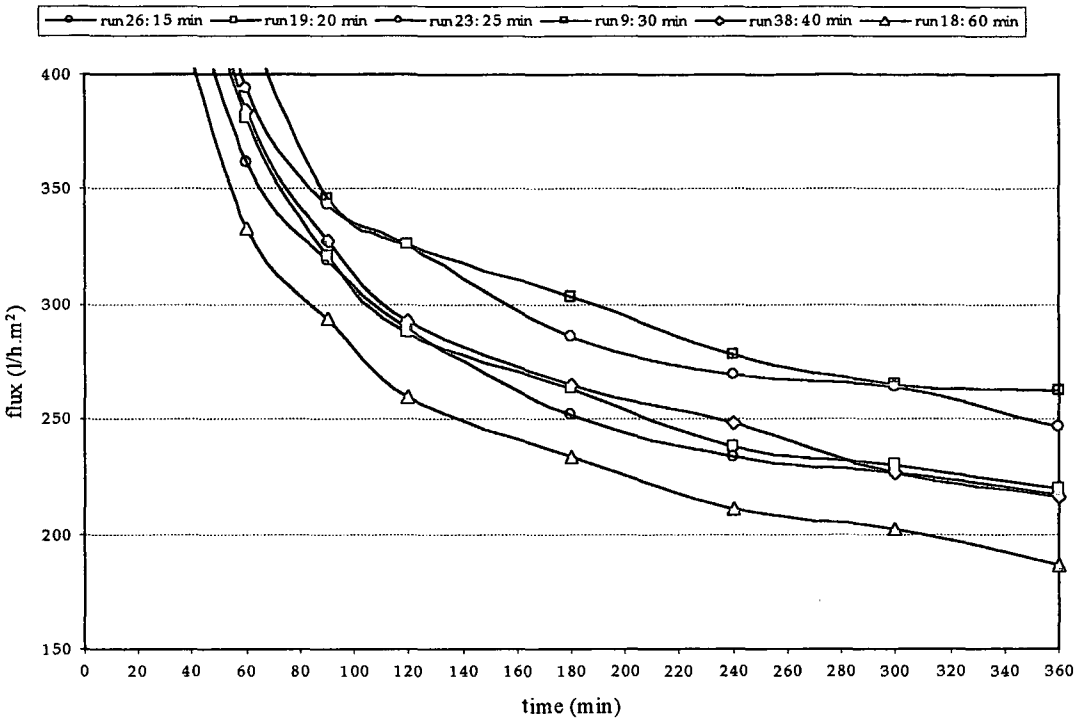

The effect of precoating time on the performance of the precoat is shown in Figure 4.3. The precoating time has a significant effect on the Production Ratio. During the first 60 minutes the Production Ratio shows a substantial increase and eventually reaches its steady state after approximately 120 minutes. Thereafter the Production Ratio-time curves are all substantially parallel.

Figure 4.3 : Figure showing the effect of the variation of precoat time on Production Ratio at a precoat concentration of 5 g/l, a velocity of 1.9 m/s, a pressure of 200 kPa and a d_{50} of 5 microns.

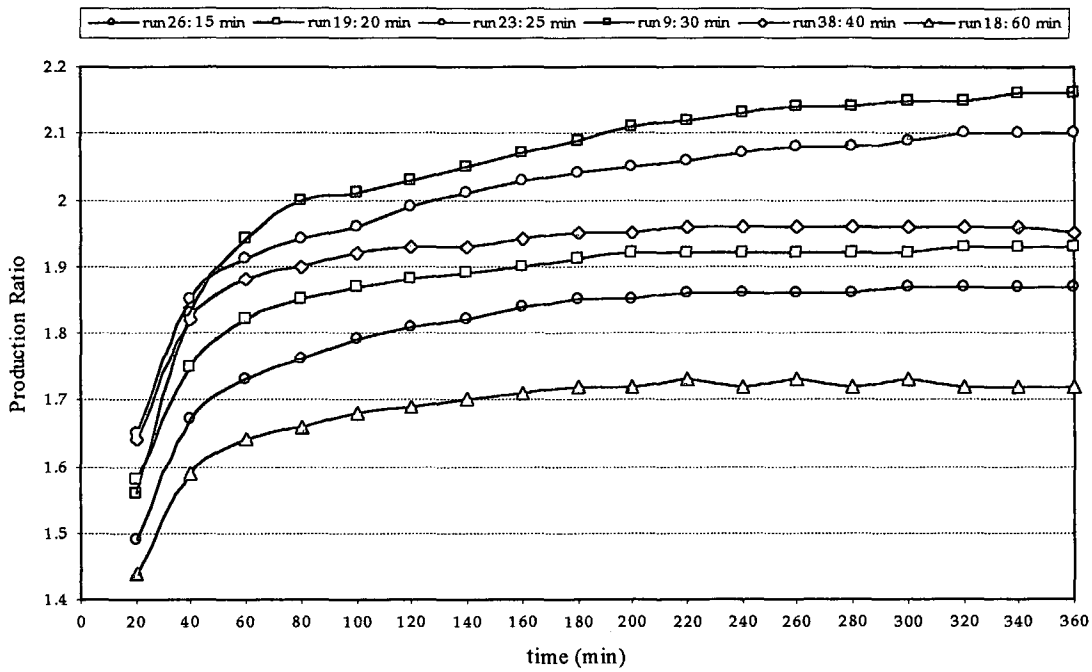

The effect of precoating time on steady state Production Ratio is depicted in Figure 4.4. Note that the steady state Production Ratio is the Production Ratio obtained after 6 hours of operation (see Chapter 3, Section 3.4). The steady state Production Ratio first increases and then decreases with precoat time. A maximum Production Ratio of 2.16 is obtained for a precoating period of approximately 30 minutes. This means that the permeate flux of the test slurry is approximately 2.2 times higher in the presence of a precoat layer than in the absence of a precoat layer. For precoating times above 30 minutes the Production Ratio declines. The decline in Production Ratio must have been due to changes in the precoat cake characteristics leading to a precoat of lower permeability. Changes in the precoat characteristics may include compression and consolidation of the precoat or infiltration of finer particles into the precoat. For precoating times below 30 minutes the Production Ratio also declines. This could be a result of the precoat layer being very thin and unstable. Nakao et al (1986) and Neytzell-de-Wilde (1988) have shown that a certain period of time was needed to obtain a stable

dynamic membrane. The experimental results obtained in this study showed that stable values of precoat flux were obtained approximately between 25 to 30 minutes.

Figure 4.4 : Figure showing the effect of the variation of precoat time on the steady state Production Ratio.

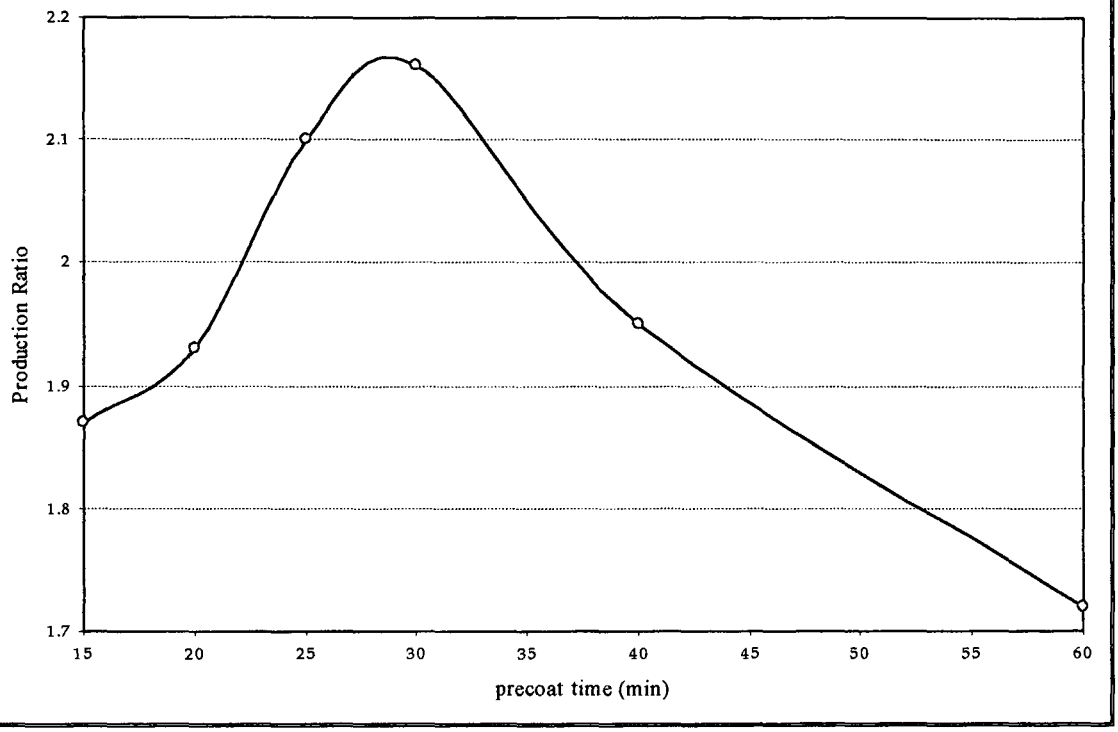

4.2.3 Effect of Precoat Velocity

The precoating time, pressure and concentration were held constant at 30 minutes, 200 kPa and 5 g/l while the precoat velocity was varied. Limestone with an average particle size of 5 microns was used for the precoat slurry. Figure 4.5(a) shows the permeate flux decline curves for various precoat velocities. Figure 4.5(a) was expanded as shown in Figure 4.5(b) so that the effect of precoat velocity could be better illustrated.

Figure 4.5(a) : Figure showing the effect of the variation of precoat velocity on flux at a precoat concentration of 5 g/l, a pressure of 200 kPa, a precoat time of 30 minutes and a d_{50} of 5 microns.

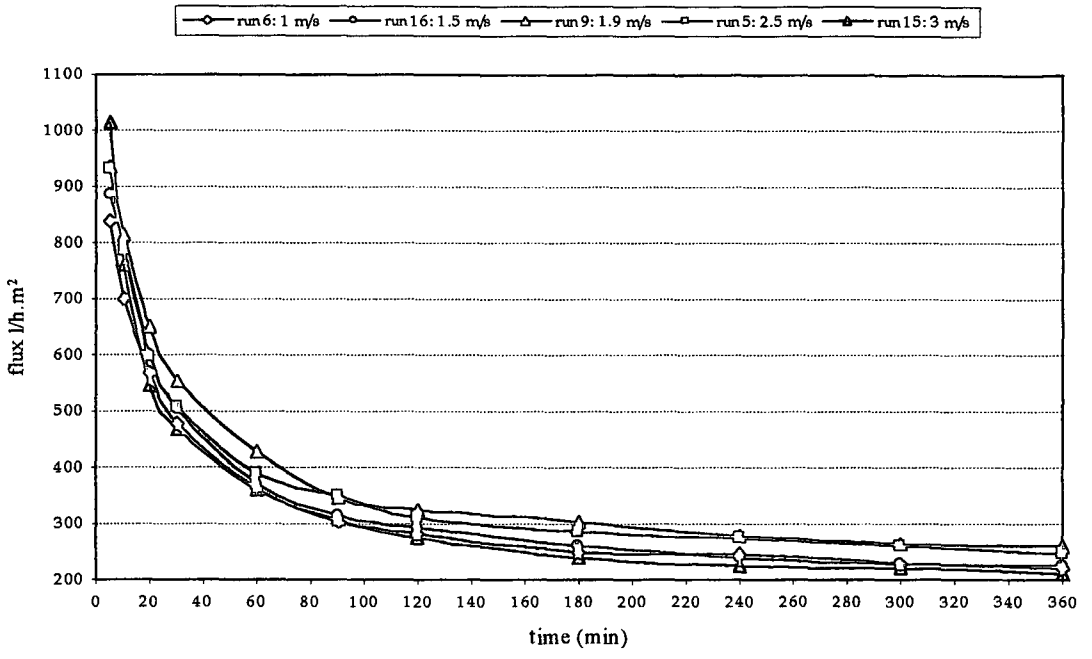

Figure 4.5(b) : Figure 4.5(a) expanded.

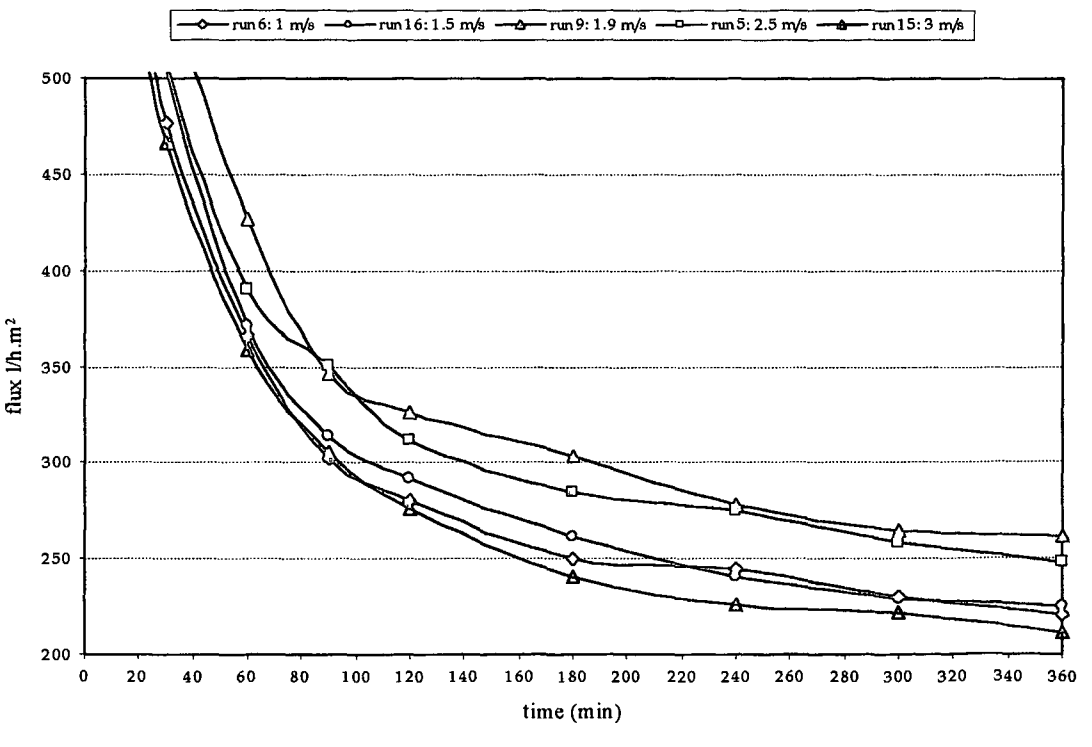

Figure 4.6 shows the effect of precoat velocity on the performance of the precoat. For precoat velocities greater than 2 m/s, the permeate flux and hence the Production Ratio decreases with increasing precoat velocity. This trend was confirmed with repeatable experiments. It implies that the precoat cake resistance increases as the precoat velocity is increased more than 2 m/s. This may be due to particle classification near the filtering surface with a preferential deposition of the finer material from the precoat feed stream. The same conclusion was reached by Fischer and Raasch (1985) for microfiltration of a calcium carbonate slurry: higher velocities limited the thickness of the deposited layer but decreased its porosity.

Figure 4.6 : Figure showing the effect of the variation of precoat velocity on Production Ratio at a precoat concentration of 5 g/l, a pressure of 200 kPa, a precoat time of 30 minutes and a d_{50} of 5 microns.

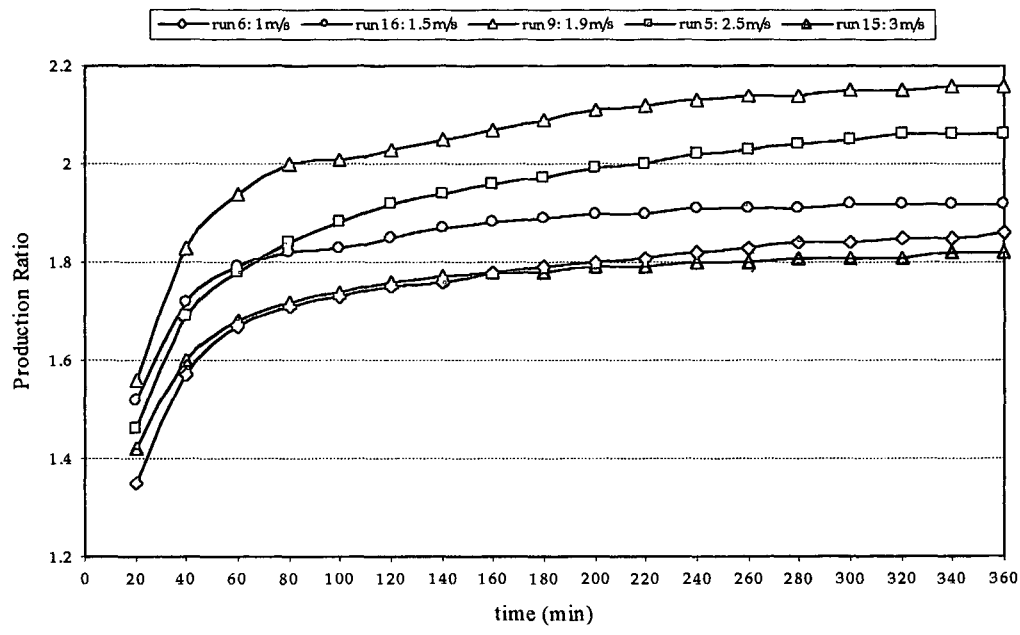

Figure 4.7 shows a plot of the steady state Production Ratio and precoat velocity. A maximum Production Ratio of 2.17 is obtained for a precoat velocity of approximately 2 m/s. The results obtained were not intuitively obvious. The beneficial effect of increasing precoat velocity seems to be reduced by precoat cakes with decreasing permeability. The effect is complex and suggest that other factors, in addition to the shear stress exerted on the precoat cake have influenced the specific resistance of the cake.

Figure 4.7 : Figure showing the effect of the variation of precoat velocity on the steady state Production Ratio.

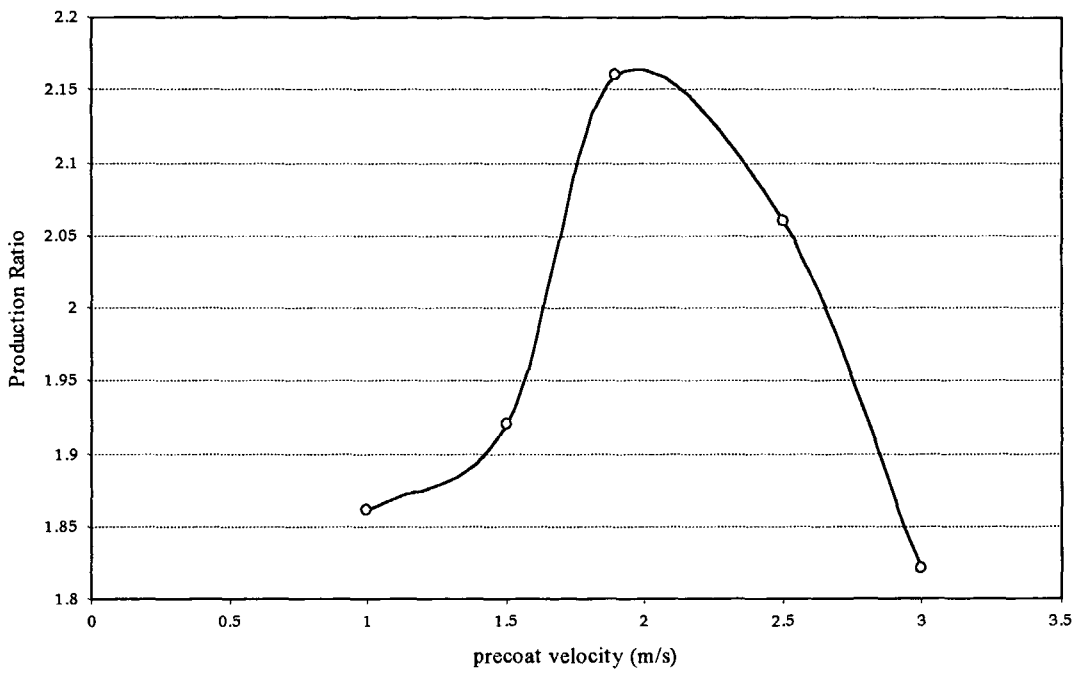

4.2.4 Effect of Precoat Pressure

Figure 4.8(a) shows the decline in permeate flux when precoat layers formed at various precoat pressures were used. Here, the runs were performed at the same precoat time, velocity, concentration and average particle size, with only the precoat pressure varying. Figure 4.8(a) is expanded as shown in Figure 4.8(b) so that the effect of precoat pressure is better illustrated.

Figure 4.8(a) : Figure showing the effect of the variation precoat pressure on flux at a precoat concentration of 5 g/l, a velocity of 1.9 m/s, a precoat time of 30 minutes and a d_{50} of 5 microns.

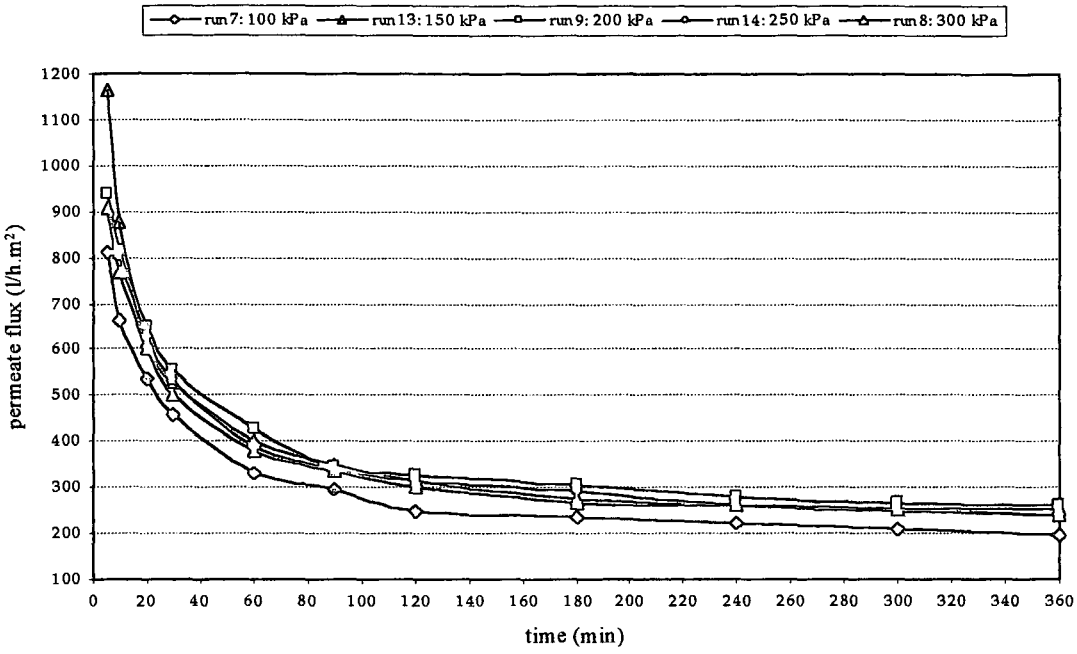

Figure 4.8(b) : Figure 4.8(a) expanded.

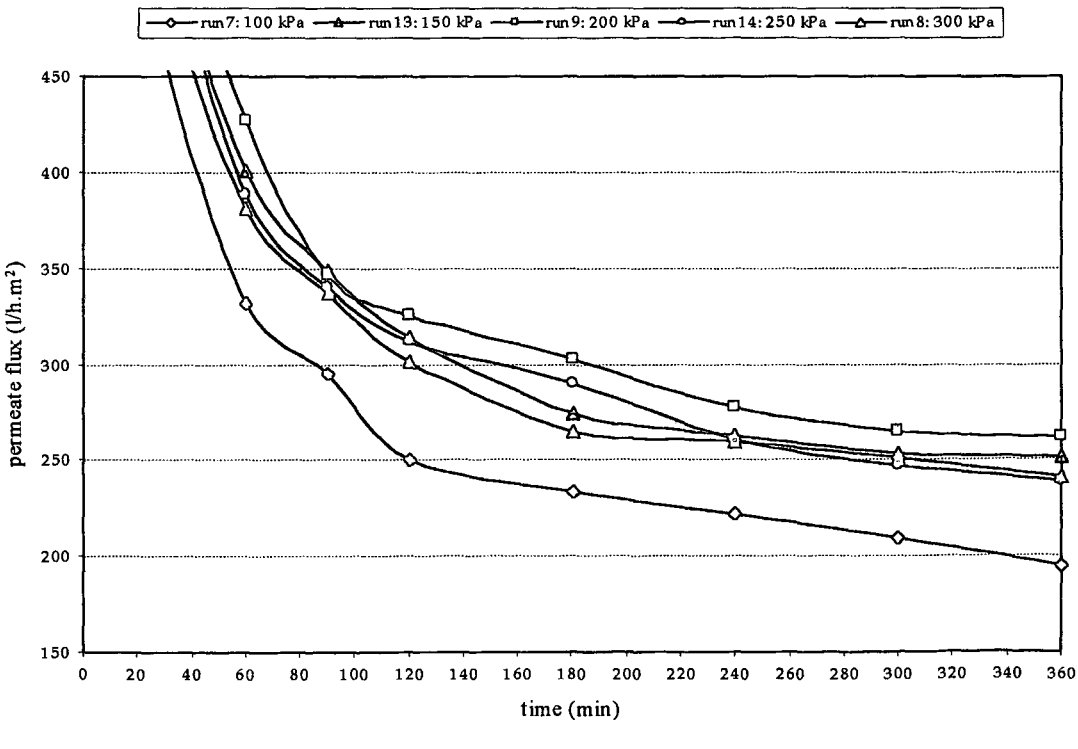

The effect of precoat pressure on the performance of the precoat is depicted in Figure 4.9. Similar to the Production Ratio-time curves obtained at different precoat times and velocities, the curves are substantially parallel once steady state has been reached. For precoat pressures from 100 kPa to 200 kPa, the trend observed is as expected. However for precoat pressures greater than 200 kPa, the Production Ratio decreases with increasing precoat pressure. This trend was confirmed with repeatable experiments. This may be due to the precoat layer being compacted to a greater degree at the higher precoat pressures, thereby reducing the porosity of the precoat layer, and hence the decrease in the Production Ratio. The same conclusion was reached by Baker et al (1985) for the microfiltration of a mineral suspension. At high pressures the specific cake resistance increased due to compressibility and the accumulation of fines following the passage of large volumes of filtrate.

Figure 4.9 : Figure showing the effect of the variation of precoat pressure on Production Ratio at a precoat concentration of 5 g/l, a velocity of 1.9 m/s, a precoat time of 30 minutes and a d_{50} of 5 microns.

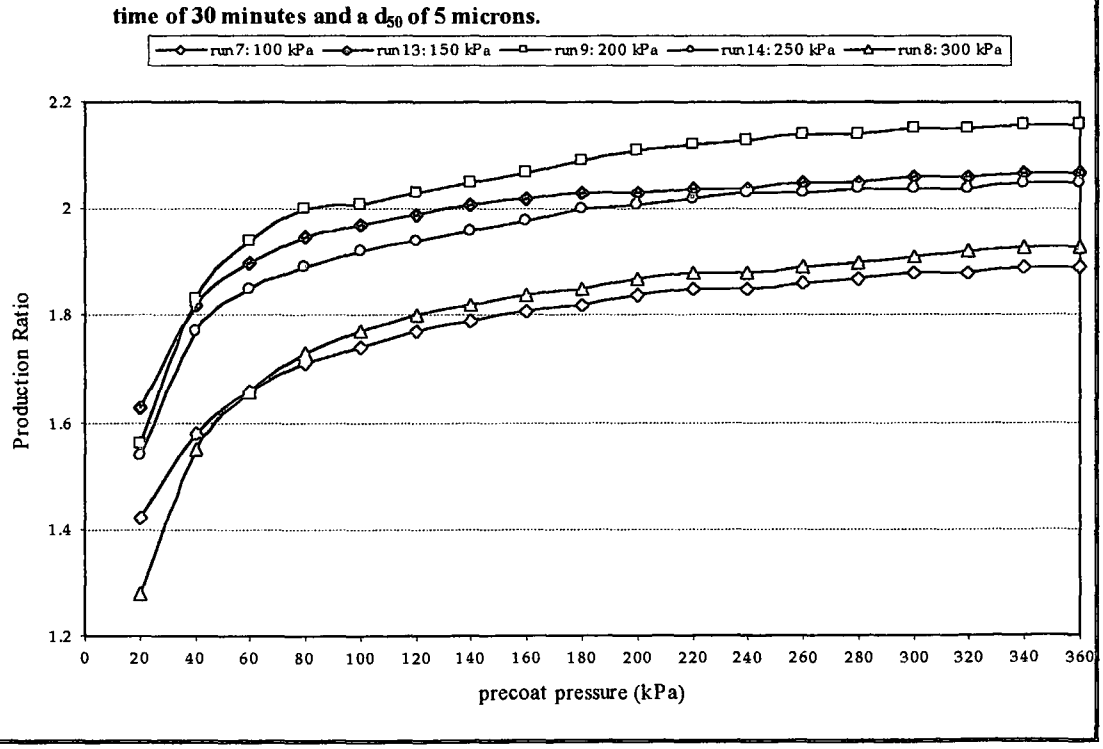

The effect of precoat pressure on steady state Production Ratio is shown in Figure 4.10. The steady state Production Ratio increases with pressure, reaches a maximum of 2.16 at approximately 200 kPa, and thereafter decreases with increasing pressure. The effect of increasing precoat pressure seems to be reduced by precoat cakes with decreasing porosity due to the accumulation of fines in the precoat and compaction of the precoat.

Figure 4.10 : Figure showing the effect of the variation of precoat pressure on the steady state Production Ratio.

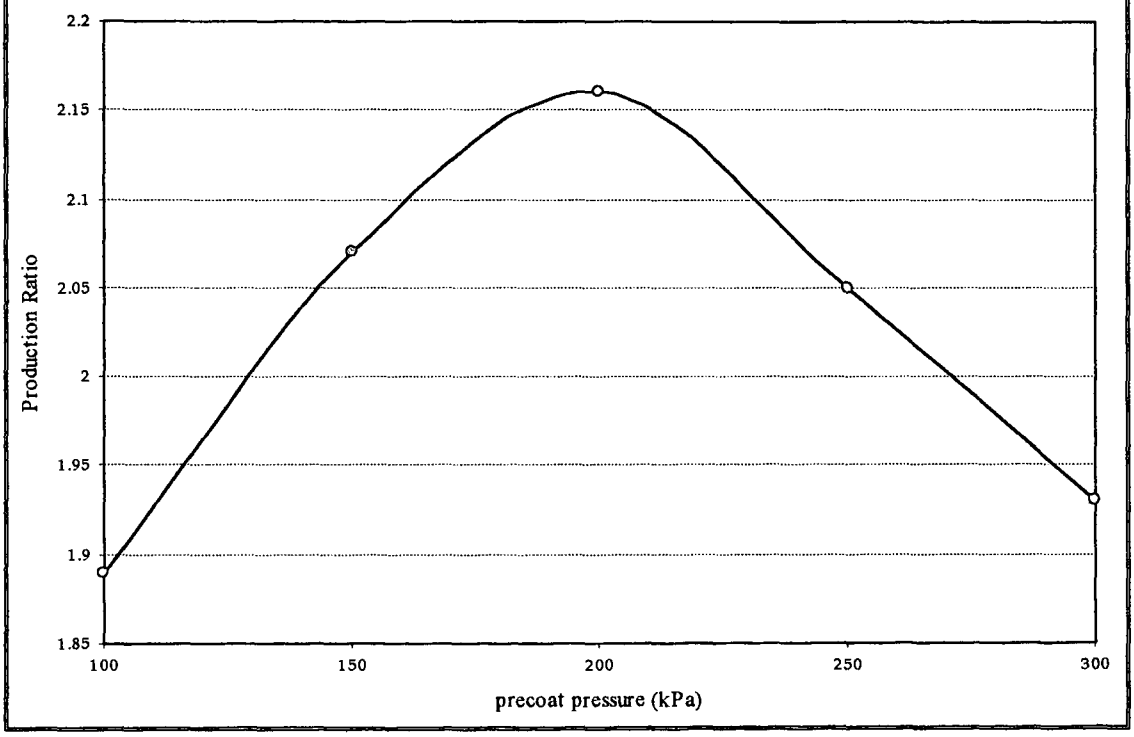

4.2.5 Effect of Precoat Concentration

Figure 4.11 shows the development of the permeate flux of the artificial feed suspension when filtered with precoat layers formed at varying concentrations. For all experiments the precoat time, velocity, pressure and average particle size were maintained constant with only the precoat concentration varying. Figure 4.12 shows the effect of precoat concentration on the Production Ratio. Once again, the Production Ratio curves are substantially parallel once steady state is reached.

Figure 4.11 : Figure showing the effect of the variation precoat concentration on flux at a precoat velocity of 1.9 m/s, a precoat pressure of 200 kPa, a precoat time of 30 minutes and a d_{50} of 5 microns.

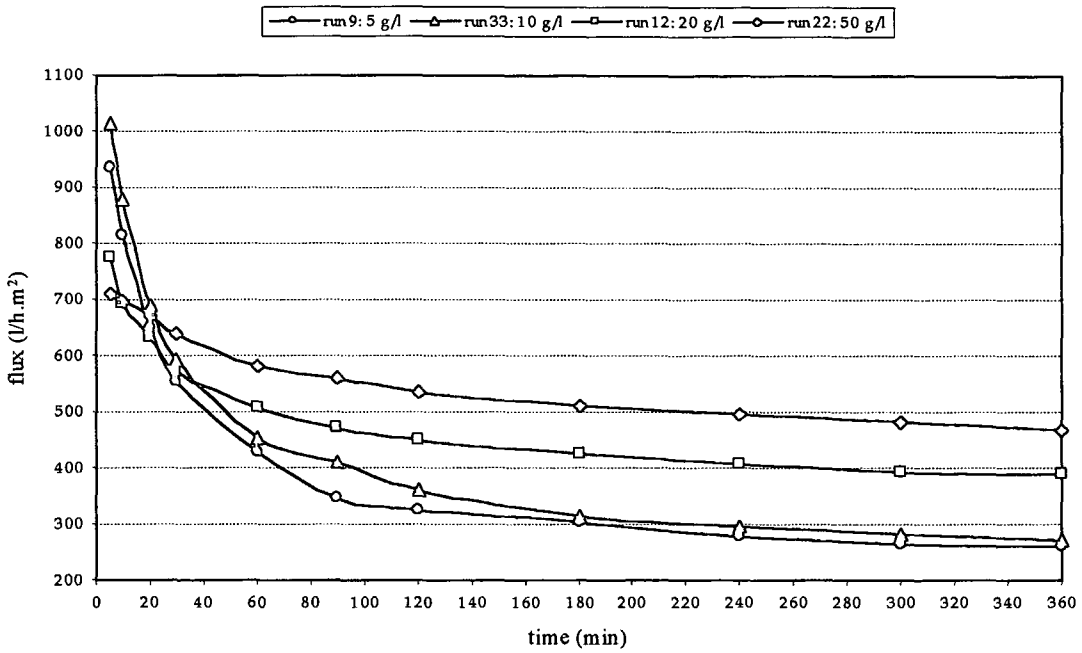

Figure 4.12 : Figure showing the effect of the variation of the precoat concentration on Production Ratio at a precoat velocity of 1.9 m/s, a pressure of 200 kPa, a precoat time of 30 minutes and a d_{50} of 5 microns.

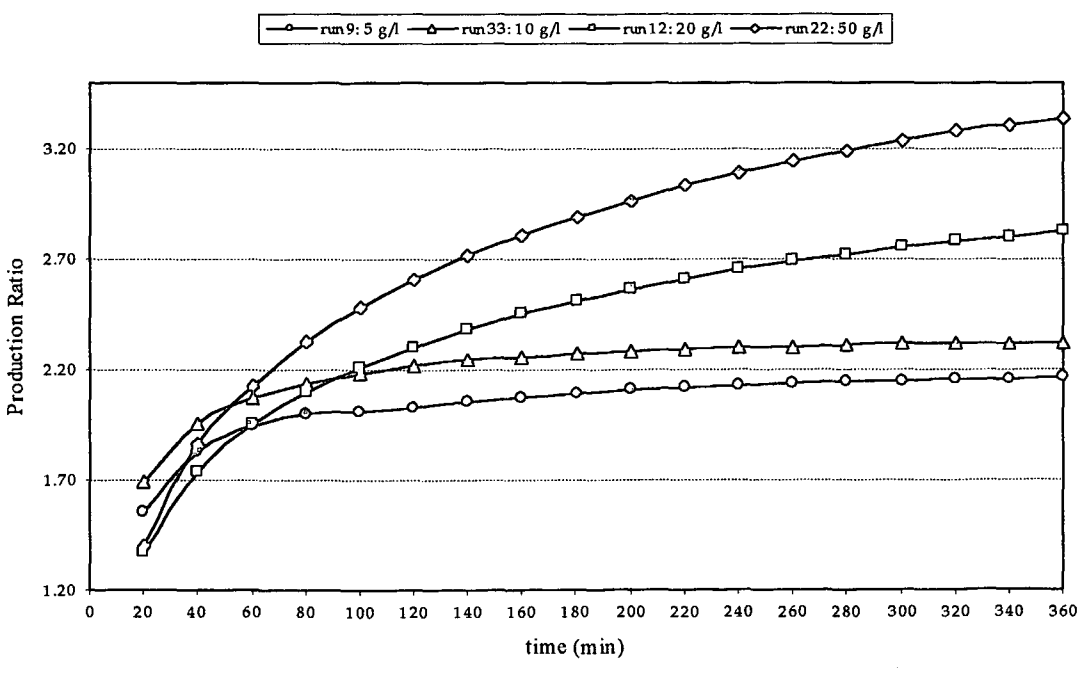

Contrary to expectations, the Production Ratio is seen to increase when filtered with precoat layers formed at increasing concentrations. This suggests that although thicker precoat layers are formed at increasing precoat concentrations, the precoat layer resistance does not increase and or the permeability of the precoat layer increases with increasing precoat concentration. Lee and Clark (1998) found in their ultrafiltration of colloidal suspensions in the unstirred dead-end filtration mode, that whilst the cake resistance increased with feed concentration, the specific cake resistance remained constant regardless of the feed concentration.

Figure 4.13 shows a plot of steady state Production Ratio vs precoat concentration. A significant dependence on concentration at the low concentrations is exhibited but at the higher concentrations the dependence weakens and the Production Ratio tends to a limiting value. It seems as if the permeability of the precoat layer increases with precoat concentration until a limiting concentration is reached.

Figure 4.13 : Figure showing the effect of the variation of precoat concentration on the steady state Production Ratio.

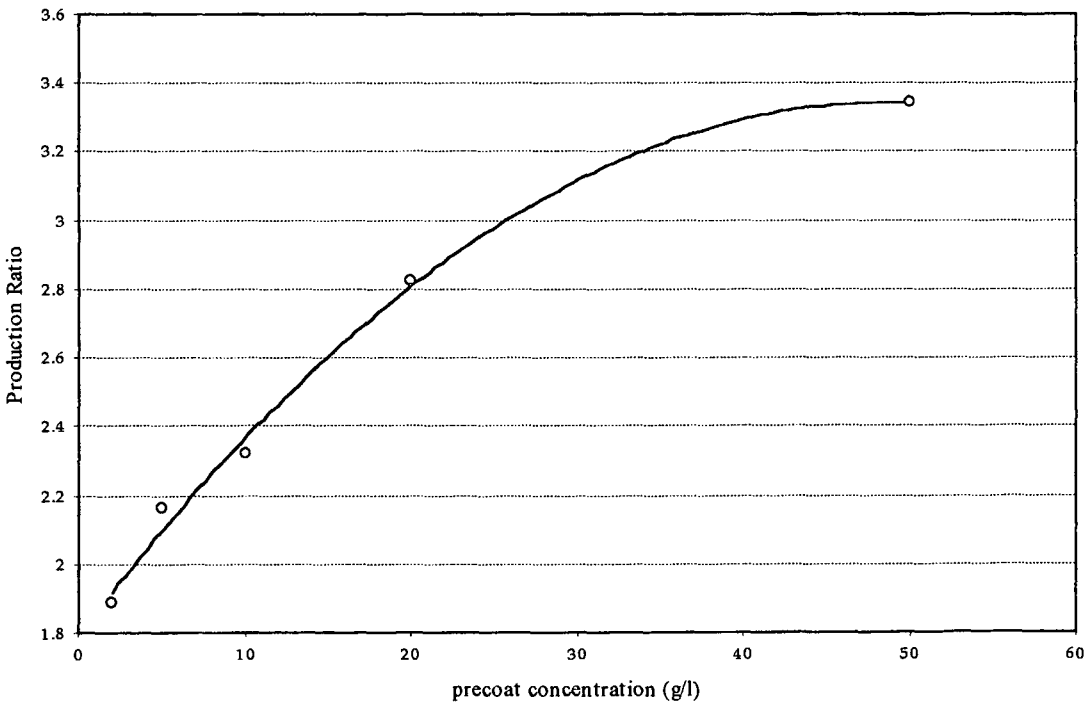

4.2.6 Effect of Average Precoat Particle Size

All experiments were performed at the same precoat time, velocity, pressure and concentration with only the average precoat particle size varying. Figure 4.14(a) shows the permeate flux of the artificial feed suspension when filtered with precoat layers formed at varying average precoat particle sizes. Figure 4.14(a) is expanded as shown in Figure 4.14(b) so that the effect of average precoat particle size is more noticeable.

Figure 4.14(a) : Figure showing the effect of the variation of average precoat particle size on flux at a precoat concentration of 5 g/l, a precoat velocity of 1.9 m/s, a precoat pressure of 200 kPa and a precoat time of 30 minutes.

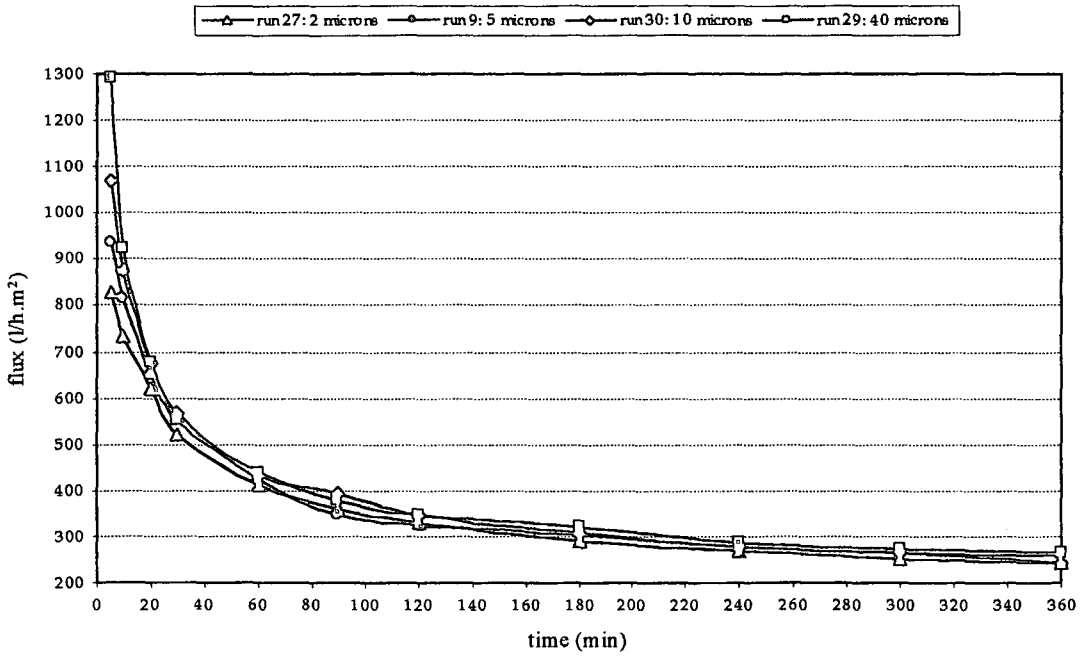

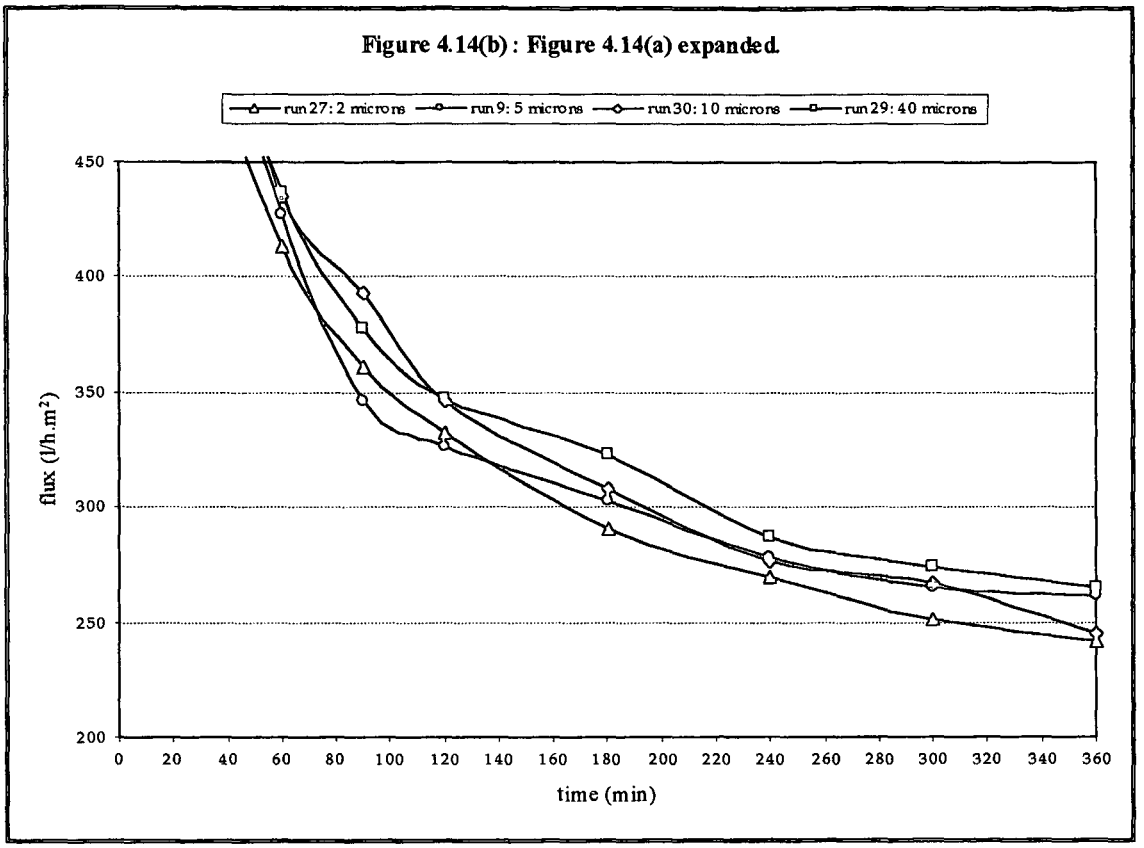

The effect of average precoat particle size on the performance of the precoat is shown in Figure 4.15. Once again the Production Ratio-time curves are substantially parallel once steady-state is reached. The permeate flux of the artificial feed suspension increases with increasing average precoat particle size. This suggests that the porosity of the precoat layer increases with particle size. Hence the resistance of the precoat layer would decrease with particle size. The same conclusion was reached by Hwang et al (1996) for microfiltration of spherical polystyrene latex particles. The cake voidage was found to increase with particle size resulting in increasing permeate fluxes. Lu et al (1993) found in their study of microfiltration of a calcium carbonate suspension, that the average specific cake resistance decreases with increasing particle size.

Figure 4.15 : Figure showing the effect of the variation of average precoat particle size on Production Ratio at a precoat concentration of 5 g/l, a velocity of 2 m/s, a pressure of 200 kPa and a precoat time of 30 minutes.

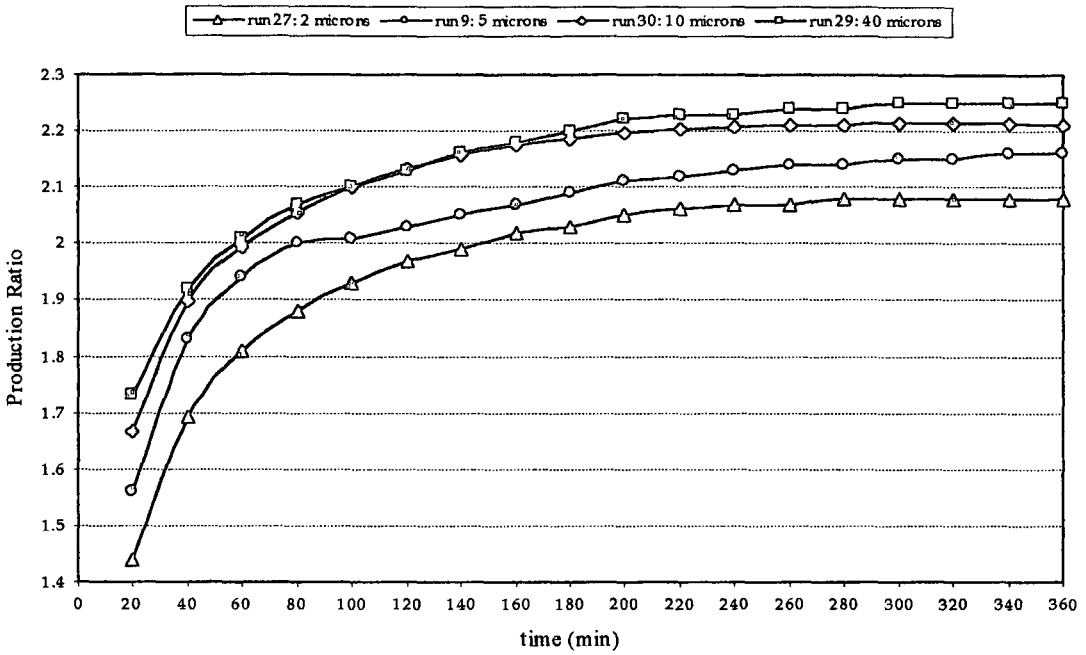

The effect of average particle size on steady state Production Ratio is depicted in Figure 4.16. As is shown in this figure, the steady state Production Ratio increases with particle size at low particle sizes, but the dependence weakens as particle size reaches higher values until finally the the steady state Production Ratio reaches a plateau. The precoat cake layer resistance for this case is significant for particles smaller than 10 μm in diameter. At the higher particle sizes the cake layer resistance is higher possibly due to particle compaction.

Figure 4.16 : Figure showing the effect of the variation of average precoat particle size on the steady state Production Ratio.

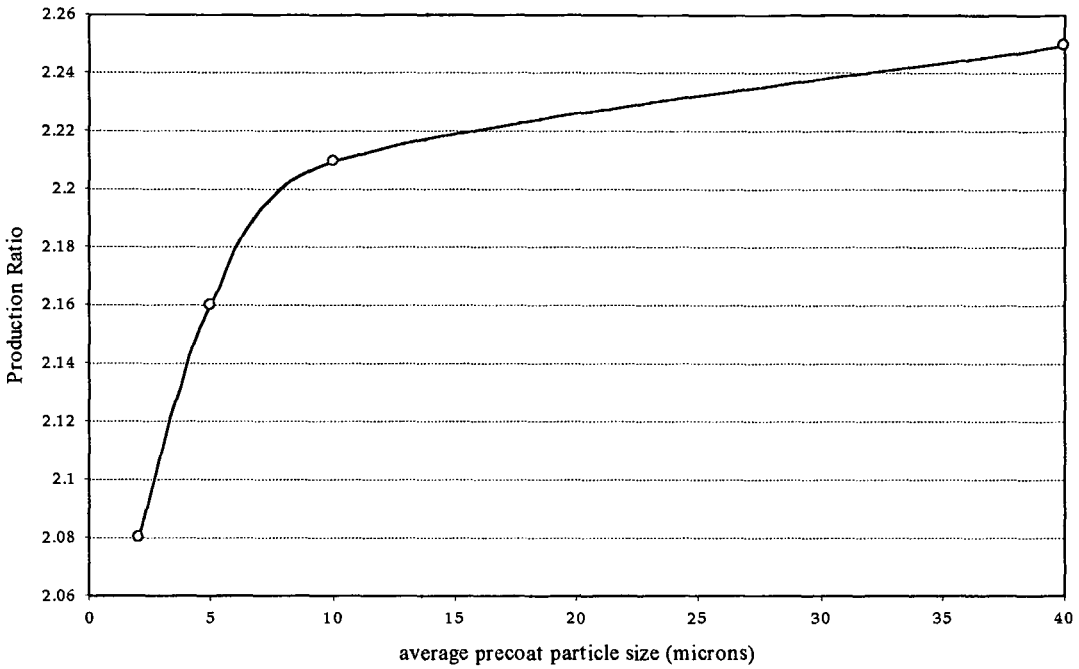

4.3 SUMMARY

The effect of the precoating variables namely precoat time, velocity, pressure, concentration and particle size, on the performance of the microfilter was investigated. Permeate flux and elapsed time were measured and recorded throughout. The flux enhancement of the precoat layer was quantified using the parameter Production Ratio. The Production Ratio is obtained by expressing the cumulative volume obtained using a precoat relative to the cumulative volume obtained without a precoat.

It was found that all of the above-mentioned precoating variables affect the performance of the microfilter. It is observed that the steady state Production Ratio goes through a maximum with an increase in precoat time, velocity and pressure. For precoat concentration and average particle size, the steady state Production Ratio increases at the low concentrations and particle sizes, but the dependence weakens as concentration

and particle size reach higher values until finally the steady state Production Ratio reaches a plateau.

The results obtained are not intuitively obvious and suggest that other factors such as hydraulic compression and preferential deposition of fines have influenced the specific resistance of the precoat layer.

Chapter 5

DISCUSSION

5.1 PRECOAT CAKE FORMATION

5.1.1 Theory of Layer Formation

Investigating the force balances at the scale of the particles provides an interpretation of the mechanisms which control particle deposition. The forces acting on a deposited particle can be simplified as shown in Figure 5.1.

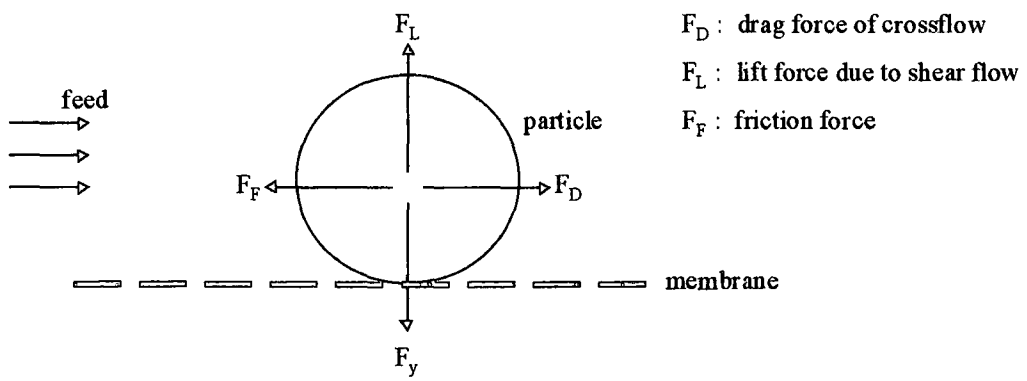

Figure 5.1 Acting forces on a single particle

5.1.2 Forces on Streaming Particle

On a streaming particle only hydrodynamic forces are acting. The fluid flow through the cake will generate frictional drag on the deposited particles. This drag would be transmitted to the surrounding particles through the contact points and be accumulated as the solid compressive forces. The drag force of the crossflow is influenced by the wall-bounded shear flow. The lift force is caused by the shearing motion of the bulk flow. The balance between the lift force and the drag force of the filtrate is largely

responsible for the transport of particles to the layer. At high filtration rates the drag force is greater for a wide particle range. This means that the particles will be transported to the layer and deposited there. Large particles experience a higher lift force and so will not be deposited. At low filtration rates the balance of the lift force and drag force of the filtrate shifts to smaller particle sizes. Therefore at low filtration rates only small particles can be deposited on the layer.

During the cake growth period particles below some critical size would deposit stably onto the cake surface or alternatively penetrate the surface, while larger particles will be sheared off. This critical particle size will decrease as the surface shear stress increases.

5.1.3 Forces on Deposited Particle

Adhesive and friction forces are acting on a deposited particle additionally to the hydrodynamic forces. The adhesive forces are caused by van der Waals forces and by electrostatic interactions. The action of a normal force (adhesive force and drag force of the filtrate flow) causes a friction force opposite to the drag force of the crossflow.

It has been found that in the lower particle range the adhesive and the friction force are larger than the corresponding hydrodynamic force [Altmann and Ripperger (1997)]. This means, that smaller particles are irreversibly attached to the layer and cannot return into the crossflow. Only large particles or particle agglomerates can be removed from the layer.

5.1.4 Growth of Layer

The suspension is pumped through the microfilter and the liquid filters through the membrane while the solids remain trapped within the microfilter. A typical flux-time curve is presented in Figure 5.2. Consistent with previously reported trends [Baker et al (1985); Pillay (1992)] the flux initially decreases rapidly, followed by a slow, almost linear decrease with time.

Figure 5.2 : Typical Flux-Time Curve for Crossflow Microfiltration

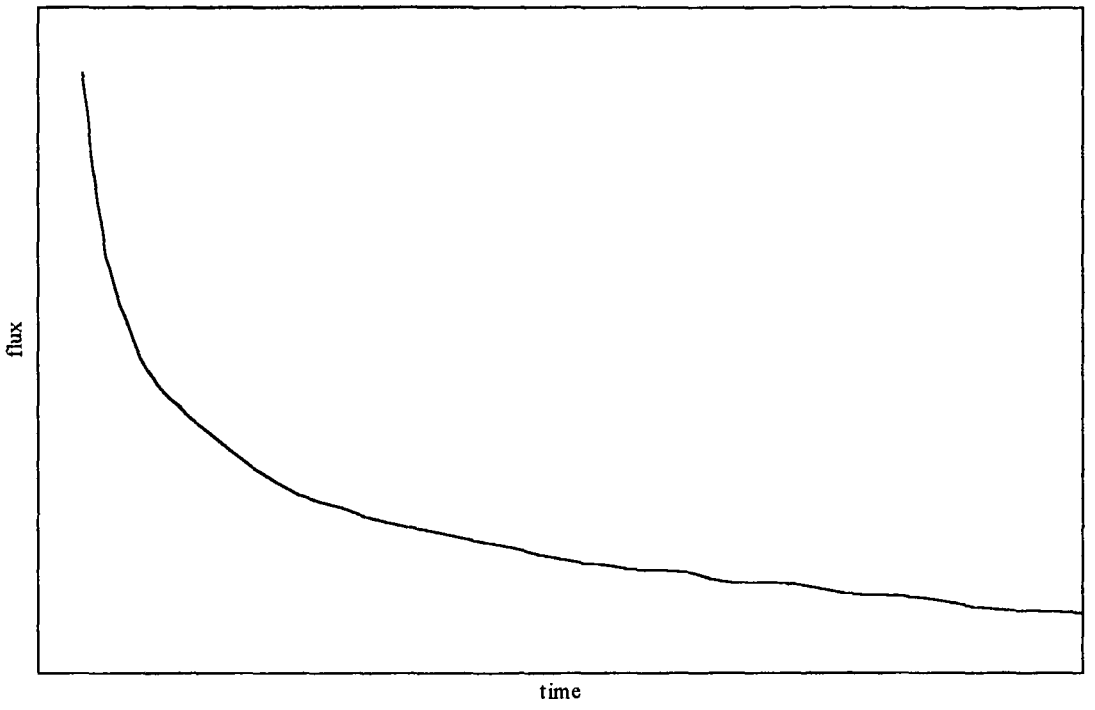

At the beginning of the process the filtration rate is determined by the pressure and resistance of the membrane. The filtrate flow causes a convective particle transport to the membrane. Particles below some critical size deposit stably onto the cake surface or alternatively penetrate the surface, while larger particles are sheared off.

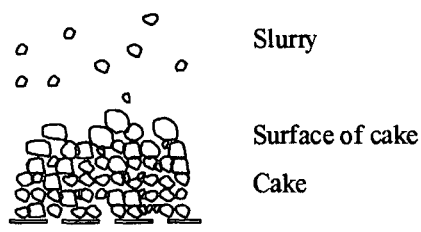

Figure 5.3 **Cross-section through surface layers of cake at an early stage of filtration**

As the layer grows the layer resistance increases and the filtration rate declines. A smaller filtration flow results in a decreased particle transport to the layer and the deposition of finer particles. This results in a slow decrease in permeability, and hence the slow long term decline in flux.

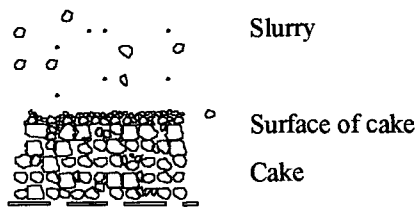

Figure 5.4 **Cross-section through surface layers of cake showing deposition of fines on the surface**

5.2 MECHANISM FOR DECLINING CAKE PERMEABILITY

The permeability of the cake depends on the voidage and specific resistance of the cake. There are 3 phenomena that contribute to the slow long term decline in flux:

1. Hydraulic compression
2. Preferential deposition
3. Fines infiltration

Hydraulic compression effect: the flow of fluid through a cake consisting of particles of a wide range of sizes could cause a rearrangement of the particulate structure, leading to a cake of decreased voidage [Pillay (1992)]. This process is termed hydraulic compression. Fluid drag forces force particles into the existing void spaces causing an irreversible collapse of the particulate structure, leading to a cake of decreased voidage.

Peferential deposition effect: the lift force on a particle is a function of the particle size. At a given velocity larger particles experience a net lift force directed away from the wall while small particles would experience a net convective force directed to the wall, leading to a cake preferentially composed of the smaller size fractions. The critical particle size will decrease as the surface shear stress increases. This means that the mean particle size of the cake will decrease as operating velocity is increased [Pillay (1992)]. Also the cake will have a radial variation in particle size distribution. On start-up the shear stress at the surface is relatively small, so the particle size distribution of the cake layers next to the wall will be close to the bulk distribution. As the cake grows, the suspension velocity in the free channel increases. Thus the mean particle size in each layer will progressively decrease on moving away from the wall reaching a minimum at the surface of the steady-state cake. So with time the permeability of the cake decreases [Fischer and Raasch (1985)].

Fines infiltration effect: in the initial stages of crossflow microfiltration particles are convected towards the cake surface by the filtrate faster than they are removed by the scouring of the surface. The particle size distribution is thus similar to the particle size distribution of the bulk slurry. Once the cake has reached its equilibrium thickness, the critical size of particles convecting to the surface decreases. Smaller particles get trapped in the void spaces between the particles and so a layer of fines deposits on the surface. Due to the smaller particle size of the fines and the lower voidage of the surface layer, the permeability of the cake decreases and the flux drops. The fines slowly migrate from the surface of the cake into spaces below and so a gradual reduction in permeability is observed. As more fines migrate into the cake, so the availability of pores reduces and the rate of flux decline decreases [Hunt et al (1987)].

5.3 THE MECHANISM OF PARTICULATE REMOVAL IN A PRECOAT LAYER

Two mechanisms, straining and collection, are important for the removal of suspended solids through a precoat layer [Treffry-Goatley et al (1987)]. The mechanisms are illustrated in Figure 5.5.

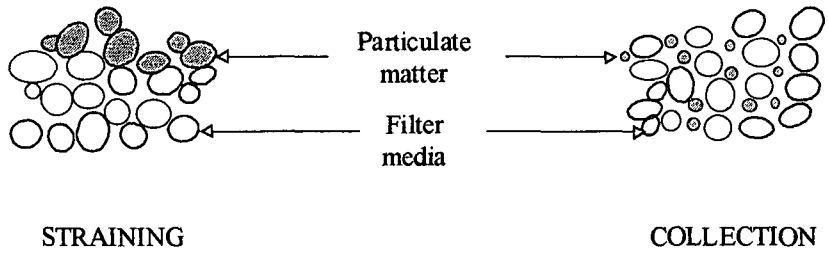

Figure 5.5 Mechanisms of particulate matter removal in a precoat layer

Straining removes particle larger than the pore openings in the precoat layer. Particles smaller than the pore openings can also be removed due to the bridging of pores. Straining can remove particles with a diameter greater than 20% of the precoat size. If straining is the controlling mechanism, head losses are expected to be high with corresponding low flux rates due to the formation of a surface mat on the precoat.

Particulate matter may also be removed through interception with the media and then attachment to the media surface. The efficiency of the interception is governed by the dimensions and velocity of the particles to be removed, the filter bed depth and mean particle size. The efficiency is improved by increasing the bed depth and decreasing the media particle diameter. In a crossflow microfilter the bed depth or precoat thickness is controlled through the operating pressure, the crossflow velocity and the precoating slurry concentration. The efficiency of attachment is determined by the degree of surface interaction between the media and the particle. It is therefore expected that permeate flux and quality can be influenced by the precoat and the conditions under which it is added.

5.4 DYNAMIC MEMBRANES

Dynamic membranes can be formed on a porous support by filtering a feed solution containing the membrane forming material. This procedure was first reported by a research group at the Oak Ridge National Laboratory in America [Marcinkowsky et al (1966)]. There are two basic types of dynamic membranes, pre-coated and self-forming dynamic membranes. The pre-coated membrane is produced by passing a solution of one or more specific components over the surface of a porous support. A self-forming membrane is a dynamic membrane in which the membrane forming materials are the same as those to be separated.

Past studies of pre-coated dynamic membranes have focused on the performance of membranes for salt rejection. The most promising membranes that have been developed are the hydrous zirconium (iv) oxide membrane and the hydrous zirconium (iv) oxide-polyacrylic acid dual layer or composite membrane [Freilich and Tanny (1978), Neytzell-de Wilde et al (1988), and Nomura and Kimura (1980)].

The following is a short and non-exhaustive review on the influence of dynamic membranes on crossflow filtration processes. A few examples are presented to highlight several conclusions.

Kishihara et al (1989) worked on clarification of sugar cane juice through a dynamic membrane formed on a porous ceramic tube. The results showed that the permeate flux of a self-forming membrane was superior to that of a conventional ultrafiltration membrane. They suggested that the formation of dynamic membranes changed the separation ranges of the original support and gave attractive values of permeate flux. However, the colour value of the permeate of the dynamic membrane was slightly inferior.

Jiraratananon et al (1997) studied the retention characteristic of self-forming dynamic membranes of pineapple juice on a porous microfiltration ceramic support. The filtration of pineapple juice by ultrafiltration alumina membrane was also carried out under the same conditions as those used by dynamic membrane for comparison.

Ultrafiltration was found to be more promising. The internal fouling resistance of the microfilter was approximately 3.5 times higher than the ultrafilter. It was suggested that the complex composition of the pineapple juice, together with the high porosity of the microfilter support were the reasons for the in-pore blockage which affected the performance of the dynamic membrane.

Ohtani et al (1991) investigated the performance of dynamic ultrafiltration membranes with fine Zr particles. The deposited layer of Zr particles produced an excellent rejection abililty as an ultrafiltration membrane and the membranes were superior in stability to conventional metal colloid membranes.

Belfort (1980) used diatomaceous earth as a precoat protective cover for the hyperfiltration of submicron colloid solutions. Filtration with the precoat produced increased permeate fluxes and rejection as compared to the filter without a precoat. Also in addition to membrane protection from fouling, there was a reduced flux-decline with the precoat than without the precoat, and the precoat cake was significantly easier to remove than the cake formed on the unprotected membrane.

The decline in flux is believed to be a major hindrance to the wide implementation of crossflow microfiltration in the water and wastewater treatment industry. Holdich and Boston (1990) investigated the application of dynamically formed membranes in the microfiltration of tap water using mineral species for the dynamic membranes. These mineral species included fluorspar, diatomite, koalin, silicate flakes and limestone.

Treffry-Goatley et al (1987) used a woven-fibre microfilter to treat a range of problematic waters. A calcium carbonate precoat was used on the tubes to treat raw surface water at a water treatment plant. The microfilter with the calcium carbonate precoat achieved water quality which was comparable to the conventional water treatment of coagulation, settling and filtration. The crossflow microfilter was also used to treat a sewage works tertiary effluent using a range of precoats. A seven fold increase in permeate flux and an improved permeate quality was obtained through the selection of the correct precoat layer.

Broom et al (1994) evaluated the application of crossflow microfiltration for the treatment of industrial waste waters containing toxic heavy metals. In this application the heavy metal precipitate provided a suitable dynamic membrane. The crossflow microfiltration was found to be a very efficient method as compared with technologies that are traditionally used for the treatment of such waters. It was also found to be much more advantageous in other aspects such as being independent upon upstream concentration variations.

Yang et al (1998) evaluated the permeability of zirconia composite membranes in a microfilter by using the membranes to separate oil-water emulsion obtained from steelworks. The zirconia composite microfiltration membrane produced attractive results and was found to be suitable to commercial application.

Shou et al (1980) investigated the feasibility of using coal bottom ash as a precoat material on a porous stainless steel support for the filtration of liquefied coal as an alternate to a commercial diatomaceous filter aid. The coal bottom ash was found to be an excellent substitute for the traditional diatomaceous filter aid. Also the economy of the process was significantly improved. The filter cake could be used as a supplemental solid fuel and the ash could be recovered for recycling.

Arora and Davis (1994) performed experiments to study the dead-end microfiltration of bovine serum albumin through asymmetric, 0.2 μm polysulfone membranes in the presence of a yeast precoat layer. The permeate flux was appreciably greater with the yeast precoat than without it. Also the yeast precoat greatly reduced the transmission of proteins which would otherwise have fouled the the membrane.

One can conclude that, in general, dynamic membranes can be formed by various materials, improve permeate fluxes and rejection, are easier to remove than the cake formed on an unprotected membrane, and reduce membrane fouling thereby increasing the life of the porous support.

5.5 DISCUSSION OF EXPERIMENTAL RESULTS

The experimental data highlight influences of the precoat process parameters: precoating time, velocity, pressure, concentration and average particle size. The results obtained are discussed with respect to existing literature data some of which are apparently contradictory, but the current data provide explanations for those contradictions and enable conclusions to be drawn.

5.5.1 Effect of Precoat Time on Production Ratio

From the precoat flux-time curve (Figure 5.6) it can be seen that the flux declines rapidly during the first 25-30 minutes. The large flux at the beginning of the filtration is only influenced by the membrane resistance. After the initial rapid decrease, a slow decrease in flux with time is observed.

Figure 5.6 : Graph showing a typical flux-time curve for the precoat. The precoat was operated at a concentration of 5 g/l, a velocity of 1.9 m/s, a pressure of 200 kPa, a precoat time of 30 minutes and a d_{50} of 5 microns.

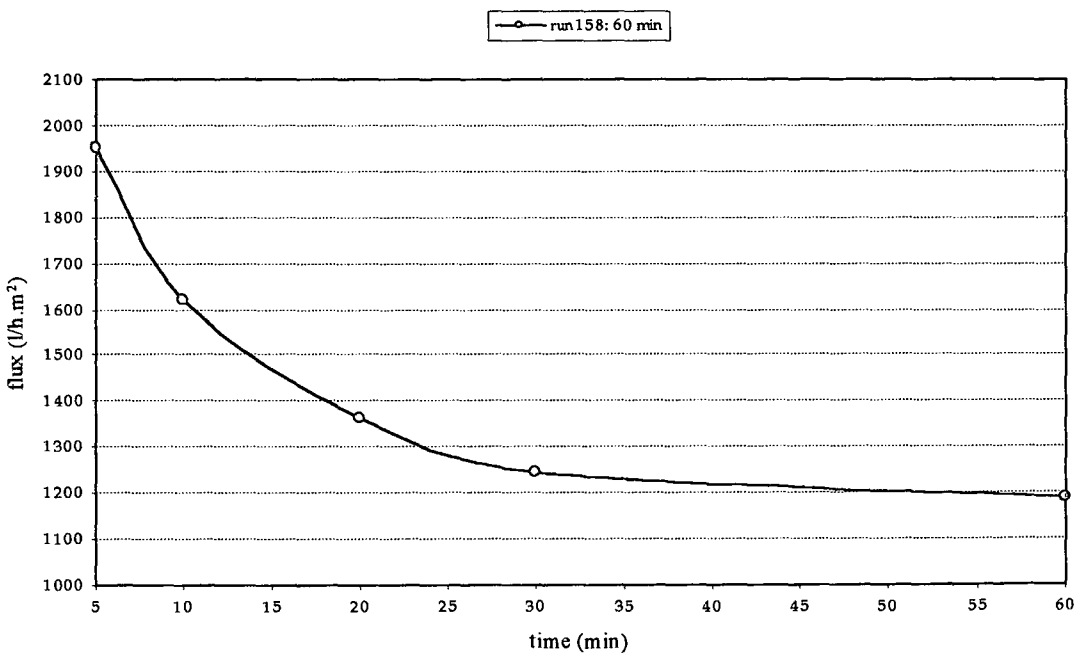

Baker et al (1985) performed experiments on a mineral slurry. Permeate flux and mass of cake deposited on the membrane was measured with time. They reported a significant drop in flux until the steady state flux was reached. Thereafter the flux continued to decline slowly. They attributed the initial drop in flux to an increase in cake mass. Once the steady state flux was obtained, the cake mass changed very slowly and was close to steady state. Measurements of the water flux before and after the experiment showed that the membrane resistance was unchanged. They attributed the steady decline in flux to continued changes in cake resistance. When the specific cake resistance was calculated, it was found that it increased with time. The increase was more significant during the steady state period. This was confirmed when they measured an increase in the fines content of the cake with time. The increase in fines would have a minor effect on cake mass. However, it would increase the specific cake resistance. Pillay (1992) also obtained similar findings in his experiments on a limestone slurry.

According to Lu and Ju (1989) the diameter of deposited particles gradually decrease due to the decay of filtration flux; therefore, the deposited particle layer will have become finer and finer during crossflow filtration. Grace (1953) and Lu et al (1993) concluded that smaller particles deposited on the cake would give a larger specific resistance to the cake.

Figure 4.4 (Chapter 4; Section 4.2) shows that the Production Ratio passes through a maximum with precoat time. The Production Ratio is a maximum at approximately 30 minutes. As can be seen from Figure 5.6 a significant drop in precoat flux is observed for approximately 25-30 minutes. Baker et al (1985) and Pillay (1992) have experimentally verified that the cake mass increases during the initial sharp decline in flux resulting in a precoat with fairly constant cake mass after approximately 25-30 minutes. For precoating times below 30 minutes, a sufficiently thick precoat layer is not formed, instead a thin unstable precoat is obtained. Particulate matter from the feed suspension which are smaller than the membrane pore openings cannot be removed by the precoat due to insufficient bridging of pores. This increases the probability of the membrane being plugged by the particulate matter thereby increasing membrane resistance.

For precoating times greater than 30 minutes a decline in Production Ratio is observed. The steady state precoat flux is obtained between 25-30 minutes so the precoat cakes formed would have reached their equilibrium thickness. Once the cake has reached its equilibrium thickness, the critical size of particles convecting to the surface decreases. Smaller particles get trapped in the void spaces between the particles and so a layer of fines deposits on the surface. Due to the smaller particle size of the fines and the lower voidage of the surface layer, the permeability of the cake decreases and the flux drops. The fines slowly migrate from the surface of the cake into spaces below and so a gradual reduction in permeability is observed. As more fines migrate into the cake, so the availability of pores reduces and the effectiveness of the precoat decreases resulting in declining Production Ratio.

5.5.2 Effect of Precoat Velocity on Production Ratio

In the work of Fordham and Ladva (1989) where the crossflow filtration of bentonite suspensions was studied by the measurement of permeate flux and measurements of steady state cake thickness. Permeate flux was observed to increase with increasing crossflow velocity, whereas the cake thickness decreased, indicating that higher shear rates reduce the cake height, and thus lowered the resistance to permeate flow.

Baker et al (1985) found that an increase in velocity results in an increase in flux and decrease in cake mass. The specific cake resistance also increased as velocity was increased. This was explained in terms of lateral migration, whereby an increase in velocity results in an increase in surface shear stress and a decrease in the size of particle capable of being captured in the cake.

Lu and Ju (1989) carried out experiments at constant pressure using a dilute calcium carbonate slurry. They measured the particle size distributions of cake formed under various filtration rates. Their results revealed that all of the particle sizes of cake are less than that of the initial liquid slurry particles. They found that a lower filtration rate decreased the size of the deposited particles. Therefore the deposited particle layer becomes finer and finer during filtration. Their results also showed an increase in the average specific resistance of the cake with an increase in the volume of filtrate

received. They indicated that this implied that smaller sized particles are deposited on the cake.

In a later paper Lu et al (1993) experimental studies showed that the particle deposition rate always decreases with an increase in crossflow velocity. They indicated that although the higher crossflow velocity gives a higher flux of particles arriving at the membrane, it also generates higher shear stress on the cake surface to give a smaller selective cut-diameter of particle deposition. As a result, it decreases the mass fraction of particles stably deposited on the membrane. They also found that for a given crossflow velocity, the deposition rate of particles decreases with a decrease in permeate flux. At the lower permeate fluxes the corresponding selective cut-diameter of the deposited particles becomes smaller, and the mass fraction of the stably deposited particles decreases.

Fischer and Raasch (1985) explained from their experimental data that an increase in slurry velocity decreases the filtration rate by the competition of cake reduction and specific cake resistance increase. They measured the particle size distribution in a cake formed under various velocities and found that most of the particles deposited on the cake came from finer parts of the initial slurry particles and that the higher velocity formed a thinner finer particles cake. They claimed that the tangent drag force due to crossflow velocity is proportional to the shear stress at the wall, τ_w, and the normal pressure force due to permeation flow is proportional to the filtration flux, q. They then found that the critical selective cut-diameter of the deposited particle is proportional to q/τ_w, which explains why higher crossflow velocity forms a finer particle cake.

Tarleton and Wakeman (1994) performed tests on calcite suspensions of mean particle sizes of 2.7 μm and 27.5 μm. With the ground suspension an increased crossflow velocity produced an improved filtration flux. Close-up video studies of the particulate layer (Wakeman, 1994) indicated that at this relatively small particle size, the thickness of the layer decreases with increasing crossflow velocity.

However, when the suspension contained a greater proportion of larger, unground particles, the filtration rate was seen to fall with increasing crossflow velocity despite a substantial thinning of the deposited layer at the higher velocities (Wakeman, 1994). This may be due to particle classification near the filtering surface with a preferential deposition of the finer material from the feed stream.

Optimisation of precoat parameters is dependent on the suspension to be filtered. Permeate flux rates and membrane retention are strongly dependent on the particle shape and size distribution of the mineral making up the dynamic membrane [Holdich and Boston (1990)].

Mackley and Sherman (1992) conducted an in situ direct observation of particle deposition during filtration of particles in the size range 125 – 180 μm using a 15 times magnification video camera, they were able to record the growth of the cake and the particle motions on the cake surface. In their crossflow filtration, the flux decreased as the crossflow velocity increases, indicating that the particles in the cake at higher crossflow velocity were smaller than at lower velocity.

The same conclusion was reached by Li et al (1998). They conducted in situ direct observation through the membrane of particle deposition in a typical microfiltration rig. Their analysis of the size distribution of the deposited particles at different crossflow velocities confirmed that the particles in the cake layer are smaller at higher crossflow velocities.

Koglin (1985) indicated that very high shear stress exerted on coagulated particles will break the structure of agglomerated particles, decrease the size of agglomerated particles and finally result in a more compact cake.

As shown in Figure 4.7 (Chapter 4; Section 4.2) the Production Ratio passes through a maximum with velocity. As the precoat velocity is increased the Production Ratio decreases. Although the higher precoat velocity gives a higher flux of particles arriving at the membrane, it also generates a higher shear stress on the precoat cake surface to

give a smaller critical diameter of particle deposition. At high filtration rates the drag force of the filtrate flow is greater for a wide particle range. That is particles will be transported to the precoat layer and deposited there. Large particles experience a higher lift force due to the shear flow, and so will not be deposited. In this way the precoat cake's flow resistance increases, even though the cake is becoming thinner. Thus a decrease in Production Ratio with an increase in velocity is observed.

The increase in the precoat specific cake resistance with an increase in crossflow velocity can also be explained in terms of a scour or erosion mechanism. The scour or erosion process preferentially dislodges large particles from the cake. At the higher velocities the precoat cakes are only a few average particles thick, and some large particles would protrude or extend above the cake surface. These larger particles would be more susceptible to scour.

Reducing precoat velocity gives lower Production Ratios. Lower precoat velocity results in lower permeate fluxes. At low filtration rates the balance of the lift force and the drag force of the filtrate shifts to smaller particle sizes, and only small particles can be deposited on the precoat layer. Therefore, the deposited particle layer becomes finer and finer during crossflow filtration. Consequently the precoat flow resistance increases, giving lower Production Ratios.

5.5.3 Effect of Precoat Pressure on Production Ratio

Baker et al (1985) studies showed that the specific cake resistance passed through a minimum at a critical pressure. The fines content of the cake also passed through a minimum at the critical pressure. At high pressures the specific cake resistance increases due to compressibility and the accumulation of fines following the passage of large volumes of filtrate. At lower pressures the lower fluxes provide insufficient convective transport of large particles.

The experimental results of Lu and Ju (1989) also revealed that a lower filtration rate induces finer deposited particles and an increase in specific cake resistance. In addition they found that a higher filtration pressure drop forms a greater thickness of cake but

gives only a slightly higher steady state filtration flux. They found that the clearance of the filter channel decreased for the case of higher pressure filtration.

Tarleton and Wakeman (1994) experimental data for a calcite suspension of mean particle size of 27.5 μm showed that only small increases in flux are obtained for quite substantial increases in filtration pressure. Filtration pressure was varied between 68 kPa and 340 kPa. When the particle size was reduced from a 50% size of 27.5 μm to 2.7 μm by grinding prior to filtration, the improvements in flux obtained by raising the filtration pressure were reduced. This phenomenon was confirmed when other suspensions containing finer particulates were filtered. They believe that the potential improvement to be gained by raising the pressure was offset by the tendency to form a higher resistance deposit. Similar effects were reported by Akay and Wakeman (1994), that a raised filtration pressure can lead to increased fouling and will not always produce an improved filtration performance.

The negative effect of a higher filtration pressure was also reported by Lee and Clark (1998) during crossflow ultrafitration of colloidal suspensions in the unstirred dead-end filtration mode. They found that the cake layer becomes more compact as the filter pressure increases, leading to a greater flux reduction. Both the cake resistance and specific cake resistance increased with increasing filtration pressure. The porosity was found to decrease with increasing filtration pressure. This implies that a higher filtration pressure results in a denser and more compact cake layer.

Romero and Davis (1988) presented a global model of crossflow microfiltration which predicts filtration flux for various operating conditions. They found that the permeate flux increases linearly with transmembrane pressure drop at low pressures, but the dependence weakens as the pressure drop reaches higher values until finally the permeate flux reaches a plateau. The explanation proposed is that, after a certain pressure driving force is reached any additional increase in filtration flux is compensated by a thickening and/or compression of the particle layer.

The cake resistance, which plays an important role in the performance of the filtration, is mainly determined by the packing porosity of the filter cake and the physical properties of particles. Hwang et al (1998) indicated that the major forces affecting the particle packing in a filter cake include the solid compressive force and the interparticle forces. The fluid flow through the filter cake will generate frictional drag on the deposited particles. This drag would be transmitted to the surrounding particles through the contact points and be accumulated as the solid compressive forces. The interparticle forces include the van der Waals forces and the electrostatic force. Hwang et al (1998) reported that when the solid compressive force is smaller than the critical value, their exists an equilibrium distance between neighbouring particles due to the electrostatic repulsive force. When the solid compressive pressure is greater than the critical value, the compressive force can overcome the repulsive barrier, and the particles will come into contact with each other. Their experimental results show that the value of average cake porosity decreases with increasing filtration pressure. They also found that the half of the cake near the filter membrane has a compact structure, and a high filtration resistance. On the other hand, the portion of the cake near the cake surface has a high porosity due to the separation of particles.

Figure 4.10 (Chapter 4, Section 4.2) shows that the Production Ratio passes through a maximum with precoat pressure. The higher pressures coincide with higher fluxes. At higher pressures a thicker precoat layer is formed. A decrease in the channel clearance of the filter results in a velocity gradient of flow on the surface, causing a higher shear stress on the cake surface, which results in a high filtration rate. Since all the experiments had the same duration the higher flux conditions would have filtered greater volumes. This would have increased the potential capture of fines in the precoat layer, leading to greater values of specific cake resistance. Also the thicker precoat layer formed, further increases the hydraulic resistance of the cake. The permeability of the precoat layer is further reduced by the increased compression of the cake. The average cake porosity decreases since the increase of solid compressive pressure results in more compression of the cake. As a result the Production Ratio is seen to decrease with increasing precoat pressure.

As precoat pressure is reduced the filtration fluxes decline. At the low fluxes the balance between the lift force and drag force shifts to smaller particles. Therefore only small particles will be deposited on the precoat layer. Consequently the precoat layer resistance increases and the Production Ratio declines.

5.5.4 Effect of Precoat Particle Concentration on Production Ratio

Wakeman (1994) found for coarser calcite suspensions, mean particle size of 27 μm, changes in the bulk concentration had little effect on either the permeate flux or growth of the particle layer thickness. That is almost identical fluxes were recorded for different suspension concentrations. Increasing the bulk concentration of finer calcite suspensions, mean particle size of 2.7 μm, led to a decrease in filtrate flux, and a corresponding increase in particle layer thickness.

It was suggested that the phenomenon of similar flux levels at different concentrations may be a consequence of the shear field generated by the crossflow stream and the membrane surface and its effect on the alignment and packing of the particles. When the feed stream is more concentrated there is a preference for filtration to occur, with particles bridging membrane pores rather than plugging them. If a more dilute suspension is considered, there is a tendency for pore plugging to occur to a more significant extent.

Lee and Clark (1998) investigated the effect of feed concentration in crossflow ultrafiltration of colloidal suspensions in the unstirred dead-end filtration mode. As expected, the higher the feed concentration, the more the permeate flux declined. Their findings also indicated that the cake resistance increases with feed concentration, while the specific cake resistance remains constant regardless of the feed concentrations. That is the feed concentration only influences the total particle mass of the cake layer and the cake layer thickness – a higher feed concentration only results in a thicker cake layer. The feed concentration does not affect the specific cake resistance.

The effect of particle concentration in the precoat slurry on the Production Ratio was studied using five different concentrations: 2 g/l, 5 g/l, 10 g/l, 20 g/l and 50 g/l. The

results are shown in Figure 4.13 (Chapter 4; Section 4.2). The steady state Production Ratio initially increases at the low concentrations and thereafter reaches a limiting value at the higher concentrations.

One would expect the steady state Production Ratio to decrease with increasing precoat concentration as the hydraulic resistance of the precoat increases due to the increase in thickness of the precoat layer. However, the results suggest that the permeability of the precoat layer increases with concentration. A possible explanation for this could be that once particles are entrapped in the pores of the precoat layer, plugging of the pores occurs. A thicker precoat layer has a higher availabilty of pores for the entrapment of particles from the feed suspension. This could be a possible explanation as to why the hydraulic resistance of the precoat due to the thickness of the layer is offset by the increasing permeability.

Also, a thicker precoat layer allows for a greater degree of surface interaction between the precoat media and particle (Treffry-Goatley 1987). The efficiency of attachment is determined by the degree of surface interaction between the precoat media and the particle.

At higher precoat concentrations the dependence of the steady state Production Ratio on concentration weakens until finally the steady state Production Ratio reaches a limiting value. A possible explanation for this could be that after a certain concentration is reached, any additional increase in permeate flux of the feed suspension is cancelled by the higher flow resistance of the precoat layer and/or compression of the precoat layer.

5.5.5 Effect of Average Precoat Particle Size on Production Ratio

Lu et al (1993) obtained a relationship between particle size and average specific cake resistance. They used different sizes of calcium carbonate to conduct their filtration tests. It was found that as the particle size is increased the average specific cake resistance decreases. Lee and Clark (1998) also reported similar findings in their ultrafiltration experiments in the unstirred dead-end filtration mode.

Hwang et al (1996) also investigated the effect of particle size on steady state permeate flux. From the results obtained in their study it has been shown that the steady state flux increases with an increase in particle size. The cake voidage was measured and it was found that the cake voidage increased as particle size is increased. This would lead to a lower cake resistance and as a result, the steady state permeate flux is higher for larger particle size.

Chen and Chiang (1998) in their ultrafiltration study investigated the relationship between the colloid particle size and the pore size of the dynamic membrane formed. They found that the smaller the particle size, the narrower is the pore size distribution of the dynamic membrane. The larger the particle size the bigger was the pore diameter of the dynamic membrane.

Tarleton and Wakeman (1993) in their studies found that at smaller particle sizes filtrate fluxes were generally lower. The presence of even a small percentage of fines in a pure calcite suspension significantly lowered flux rates.

Romero and Davis (1988) global model of crossflow microfiltration shows a strong dependence of filter performance on particle size. The model predicts that permeate flux increases with an increase in particle size. Larger particles undergo sufficient diffusion to keep the entire cake layer flowing throughout the length of the filter. Smaller particles form a stagnant layer at some position in the filter, causing a decrease in permeate flux. The rate at which particles are deposited by convective motion of permeate through the membrane is balanced by the back-diffusion of particles away from the layer. Particles in the concentrated layer are lifted by the shearing motion of the bulk suspension. This results from hydrodynamic interactions of particles in the concentrated layer due to the shear flow of the layer. A particle in a shear field will tumble over other nearby particles and thereby undergo a series of displacements from the bulk-average streamline. This results in a net migration of particles from a region of high concentration to a region of low concentration. Because the smaller particles have a lower hydrodynamic diffusion coefficient than larger particles, the small-particle suspension is more tightly packed and cannot flow as easily. It is unable to provide

sufficient shear to drive the small deposited particles away from the membrane. Thus smaller particles form a thicker stagnant cake layer which causes a decline in filter performance. Larger particles have higher diffusion coefficients and would aid in the back-diffusion of the smaller particles.

As shown in Figure 4.16 (Chapter 4; Section 4.2) the Production Ratio increases linearly with an increase in precoat particle size at low particle sizes. At higher particle sizes the dependence of Production Ratio on particle size weakens until finally the Production Ratio reaches a plateau. As the particle size is increased the voidage of the precoat layer increases and the average specific cake resistance decreases. The permeability of the precoat increases giving higher Production Ratios. At the higher particle sizes, the effect on Production Ratio becomes insignificant. A possible explaination for this could be that after a certain particle size is reached, any additional increase in permeate flux is compensated by a thickening and/or compression of the precoat layer.

5.5 SUMMARY

The shape of the characteristic flux-time curve may be attributed to two phenomena. On start-up, the flux decreases rapidly, due to a rapid increase in cake thickness. Thereafter, the cake becomes limited to some steady state thickness, but changes in the cake characteristics lead to a slow long-term decline in flux.

Three phenomena that are likely to cause changes in the cake characteristics are hydraulic compression of the cake, the preferential deposition effect and the fines infiltration effect. These phenomena are mainly due to the presence of a wide size range of particles in the suspension.

Hydraulic compression occurs when fluid drag forces cause an irreversible collapse of the particulate structure, leading to a cake of decreased voidage. The preferential deposition effect concerns the deposition of smaller particles onto the cake, in preference to the larger size fractions. The fines infiltration effect concerns the

progressive infiltration of very fine particles into the existing cake structure. The above phenomena change the voidage and hence the pemeability of the cake.

Possible reasons and explanations were discussed for the individual effects of the precoating operating variables on the Production Ratio. It has been shown that the steady state Production Ratio goes through a maximum with an increase in precoat time, velocity and pressure. As the precoating period is increased the subsequent collection of fines within the precoat layer results in higher specific cake resistance and a decline in the steady state Production Ratio. As the precoating period is reduced, it is thought that a thin unstable precoat is formed resulting in the membrane being fouled, hence lower Production Ratios.

The beneficial effect of increasing precoat velocity is reduced by the tendency to form precoats of increasingly high specific resistance resulting in lower Production Ratios. This can be explained in terms of the lateral migration, whereby an increase in velocity results in a decrease in the size of particle capable of being captured in the cake. Alternatively a scour or erosion mechanism may cause preferential dislodgement of larger particles which protrude above the precoat surface. At low velocities the lower fluxes provide insufficient convective transport of large particles to overcome the effects of lateral migration. Preferential deposition of fines produces a precoat with high specific resistance, hence lower Production Ratios.

At high pressures the specific resistance of the precoat increases due to compressibility and the accumulation of fines following the passage of large volumes of filtrate, thus declining Production Ratios. At low pressures the preferential deposition of fines produces precoats with high values of specific resistance resulting in lower Production Ratios.

For precoat concentration and average particle size it was found that initially the Production Ratio increases at the low concentrations and particle sizes and eventually tends to a limiting value at high concentrations and particle sizes. At the low concentrations it appears that the increasing hydraulic resistance of the precoat due to

the thicker precoat layer is offset by the increasing permeabilty of the precoat. An explanation for this could not be found. At the higher precoat concentrations the higher permeate fluxes could be compensated by the thickening and/or compression of the precoat layer.

In the case of varying particle size, as the particle size is increased the voidage of the precoat layer increases and the average specific cake resistance decreases. The permeability of the precoat increases giving higher Production Ratios. After a certain particle size is reached, any additional increase in permeate flux could be compensated by a thickening and/or compression of the precoat layer.

Chapter 6

CONCLUSION AND RECOMMENDATIONS

This study has concerned investigations into the effect of precoating operating variables (namely precoating time, velocity, pressure and concentration) on the performance of the microfilter in order to establish an optimal precoating strategy. The correlation between precoat particle size and performance of the microfilter was also investigated in order to gain a better understanding as to why precoats enhance performance of the microfilter.

The degree to which the flux is enhanced by the precoat layer had to be quantified. Since the filtration system does not attain a true steady state as there is a slow continuous decline in flux, the flux could not be used to determine the performance of the precoat layer. The flux enhancement was quantified by expressing the cumulative volume obtained using a precoat relative to the cumulative volume obtained without a precoat. The ratio is expressed using a parameter Production Ratio. The Production Ratio remains constant after 6 hours of operation, so it can be said with certainty that the Production Ratio obtained after 6 hours will be the Production Ratio if the microfilter is operated for more than 6 hours.

The steady state Production Ratio passes through a maximum with increasing precoat time. As the precoating period is increased the subsequent collection of fines within the precoat layer results in higher specific cake resistance and a decline in the steady state Production Ratio. As the precoating period is reduced, it is thought that a thin unstable precoat is formed. This would increase the probability of the membrane being plugged by the particulate matter thereby increasing membrane resistance, leading to lower steady state Production Ratios.

The steady state Production Ratio has been shown to pass through a maximum with increasing precoat velocity. The beneficial effect of increasing precoat velocity is reduced by the tendency to form precoats of increasingly high specific resistance resulting in lower Production Ratios. This can be explained in terms of the lateral migration, whereby an increase in velocity results in a decrease in the size of particle capable of being captured in the cake. Alternatively a scour or erosion mechanism may cause preferential dislodgement of larger particles which protrude above the precoat surface. At low velocities the lower fluxes provide insufficient convective transport of large particles to overcome the effects of lateral migration. Preferential deposition of fines produces a precoat with high specific resistance, hence lower Production Ratios.

The Production Ratio also passes through a maximum with increasing precoat pressure. At high pressures the specific resistance of the precoat increases due to compressibility and the accumulation of fines following the passage of large volumes of filtrate, thus declining Production Ratios. At low pressures the preferential deposition of fines produces precoats with high values of specific resistance resulting in lower Production Ratios.

For the effect of precoat concentration it was found that initially the Production Ratio increases at the low concentrations and eventually tends to a limiting value at high concentrations. At the low concentrations it appears that the increasing hydraulic resistance of the precoat due to the thicker precoat layer is offset by the increasing permeabilty of the precoat. An explanation for this could not be found. At the higher precoat concentrations the higher permeate fluxes could be compensated by the thickening and/or compression of the precoat layer.

For the effect of precoat particle size it was shown that the Production Ratio increases with an increase in particle size at low particle sizes. At higher particle sizes the dependence of Production Ratio on particle size weakens until finally the Production ratio reaches a plateau. As the particle size is increased the voidage of the precoat layer increases and the average specific cake resistance decreases. The permeability of the precoat increases giving

higher Production Ratios. After a certain particle size is reached, any additional increase in permeate flux could be compensated by a thickening and/or compression of the precoat layer.

The results obtained were not inituitively obvious. The highest velocity and pressure are not necessarily the best operating conditions. Hydraulic compression of the precoat, preferential deposition of fines and the fines infiltration effect have affected the permeability of the precoat layer. The optimum precoating conditions obtained in this study using limestone as the precoating material are a precoat time of approximately 30 minutes, a precoat velocity of 2 m/s, a precoat pressure of 200 kPa, a precoat concentration of 5 g/l and an average particle size of 10 microns. At these operating conditions the production increased 2.2 times.

Recommendations

1. The results reported in this investigation were obtained for one type of precoat and artificial feed suspension. The magnitude of the various effects observed will depend uniquely on the particle shape and size, size distribution and nature of the solids being filtered. Further experiments could be performed on the system that was used in this study using a range of precoating materials. Commonly encountered mineral solutions such as diatomeous earth (dendrite particle shape) and koalin (platelet particle shape) could possibly be used to form precoats. This would allow for the evaluation of the effect of particle shape and size distribution on the filtration.

2. A more fuller understanding of the cake structure formed under various opearting conditions is required. The structure of cake layers is thought to change continuously during microfiltration due to factors such as particle capture/loss and consolidation. The filtration experiments by themselves is not sufficient as reasoning is inferred rather than directly observed. Experimentation needs to be performed whereby the cake is allowed to form under different steady operating conditions. After the nominated time, the membrane module can be isolated, the membrane can be removed and cut open; and a

post mortem of the cake layer can be done using an electron microscope. This might give further insight into how precoats might be manipulated in order to maximise the production.

3. Also experiments could be performed on the system using a different feed suspension. This would establish whether the trends observed in this study hold true for other systems as well. This could be very useful in preparing precoats for treating raw and waste water.

REFERENCES

ALTMANN, J. and RIPPERGER, S. (1997), **Particle Deposition and Layer Formation at the Crossflow Microfiltration**, *Journal of Membrane Science*, **124**, pp. 119-128

AKAY, G. and WAKEMAN, R.J. (1994), **Crossflow Microfiltration Behaviour of a Double Chain Surfactant Dispersion in Water: Part 1: The Effect of Process and Membrane Characteristics on Permeate Flux and Surfactant Rejection**, *Chemical Engineering Science*, **49(2)**, pp. 271

ARORA, N. and DAVIS, R.H. (1994), **Yeast Cake Layers as Secondary Membranes in Dead-End Microfiltration of Bovine Serum Albumin**, *Journal of Membrane Science*, **92**, pp. 247-256

BAKER, R.J., FANE, A.J., FELL, C.J.D. and YOO, B.H. (1985), **Factors Affecting Flux in Crossflow Filtration**, *Desalination*, **53**, pp. 81-93

BELFORT, G. (1980), **Artificial Particulate Fouling of Hyperfiltration Membranes IV. Dynamic Protection from Fouling**, *Desalination*, **34**, pp. 159-169

BROOM, G.P., SQUIRES, R.C., SIMPSON, M.P.J. and MARTIN, I. (1994), **The Treatment of Heavy Metal Effluents by Crossflow Microfiltration**, *Journal of Membrane Science*, **87**, pp. 219-230

BUCKLEY, C.A., NEYTZELL-DE WILDE, F.G., TOWNSEND, R.B., CAWDRON, M.P.R., STEENKAMP, C., SIMPSON, M.P.J. and BOSCHOFF, T.L. (1988), **Dynamic Membrane Treatment of Wool Scouring Effluents**, *Proceedings of the Symposium on Advances in Reverse Osmosis and Ultrafiltration, Toronto*, pp. 317-333

CHANG, D.J., HSU, F.C. and HWANG, S.J. (1995), **Steady-State Permeate Flux of Cross-Flow Microfiltration**, *Journal of membrane Science*, **98**, pp.97-106

CHEN, C.C. and CHIANG, B.H. (1998), **Formation and Characteristics of Zirconium Ultrafiltration Dynamic Membranes of Various Pore Sizes**, *Journal of Membrane Science*, **143**, pp. 65-73

CHUDACEK, M.W. and FANE, A.G. (1984), **The Dynamics of Polarisation in Unstirred and Stirred Ultrafiltration**, *Journal of Membrane Science*, **21**, pp. 145-160

DAVIS, R.H. and BIRDSELL, S.A. (1987), **Hydrodynamic Model and Experiments for Crossflow Microfiltration**, *Chemical Engineering Communications*, **49**, pp. 217-234

FANE, A.G. (1984), **Ultrafiltration of Suspensions**, *Journal of Membrane Science*, **20**, pp. 249-259

FISCHER, E. and RAASCH, J. (1985), **Cross-Flow Filtration**, *German Chemical Engineering*, **8**, pp. 211-216

FORDHAM, E.J. and LADVA, H.K.J. (1989), **Cross-Flow Filtration of Bentonite Suspensions**, *PhysicoChemical Hydronamics*, **11**(4), pp. 411-439

FREILICH, D. and TANNY, G.B. (1978), **Hydrodynamic and Microporous Support Pore Size Effects on the Properties and Structure of Dynamically Formed Hydrous Zr(IV)-Polyacrylate Membranes Membranes**, *Desalination*, **27**, pp. 233-251

GASSEL, T.J. and RIPPERGER, S. (1985), **Crossflow Microfiltration in the Process Industry**, *Desalination*, **53**, pp. 373-387

GOURGUES, C., AIMAR, P. and SANCHEZ, V. (1992), **Ultrafiltration of Bentonite Suspensions with Hollow Fibre Membranes**, *Journal of Membrane Science*, **74**, pp. 51-69

GRACE, H.P. (1953), **Resistance and Compressibilty of Filter Cakes**, *Chemical Engineering Progress*, **49**, pp. 303-318, 367-376

HEERTJIES, P.M. (1957), **Studies in Filtration, Blocking Filtration**, *Chemical Engineering Science*, **6**, pp. 190-203

HOLDICH, R.G. and BOSTON, J.S. (1990), **Microfiltration using a Dynamically Formed Membrane**, *Filtration and Separation*, **May/June**, pp. 184-187

HUNT, J.W., BROUCKAERT, C.J., RAAL, J.D. and TREFFRY-GOATLEY, K. (1987), **The Unsteady-State Modelling of Cross-flow Microfiltration**, **,

HUNT, J.W., TREFFY-GOATLEY, K., FLEMMER, R.L.C., JAAL, J.D. and BUCKLEY, C.A. (1987), **A Mathematical Model of Steady-State Cross-Flow Microfiltration in a Woven Hose Support**, *Desalination*, **61**, pp. 187-200

HWANG, K.J., LIU, H.C. and LU, W.M. (1998), **Local Properties of Cake in Cross-Flow Microfiltration of Submicron Particles**, *Journal of Membrane Science*, **138**, pp. 181-192

HWANG, S.J.,CHANG, D.J. and CHEN, C.H. (1996), **Steady State Permeate Flux for Particle Cross-Flow Filtration,** *The Chemical Engineering Journal*, **61**, pp. 171-178

JIRARATANANON, R., UTTAPAP, D. and TANGAMORNSUKSUN, C. (1997), **Self-forming Dynamic Membrane for Ultrafiltration of Pineapple Juice,** *Journal of membrne Science*, **129**, pp. 135-143

KISHIHARA, S.,TAMAKI, H., FUJII, S. and KOMOTO, M. (1989), **Clarification of Technical Sugar Solutions Through a Dynamic Membrane Formed on a Porous Ceramic Tube,** *Journal of Membrane Science*, **41**, pp. 103-114

KOGLIN, B. (1985), **Influence of Agglomeration on Filterability of Suspensions,** *German Chemical Engineering*, **8**, pp. 217-223

LEE, Y. and CLARK, M.M. (1998), **Modeling of Flux Decline During Crossflow Ultrafiltration of Colloidal Suspensions,** *Journal of Membrane Science*, **149**, pp. 181-202

LI, H., FANE, A.G., COSTER, H.G.L. and VIGNESWARAN, S. (1998), **Direct Observation of Particle Deposition on the Membrane Surface During Crossflow Microfiltration,** *Journal of Membrane Science*, **149**, pp. 83-97

LU, W.M., HWANG, K.J. and JU, S.C. (1993), **Studies on the Mechanism of Cross-Flow Filtration,** *Chemical Engineering Science*, **48**(5), pp. 863-872

LU, W.M. and JU, S.C. (1989), **Selective Particle Deposition in Crossflow Filtration,** *Separation Science and Technology*, **24**(7 & 8), pp. 517-540

MACKLEY, M.R. and SHERMAN, N.E. (1992), **Cross-Flow Cake Filtration Mechanisms and Kinetics,** *Chemical Engineering Science*, **47**, pp.3067-3084

MARCINKOWSKY, A.E., PHILIPS, K.A., JOHNSON, H.O. and SHON, J.S. (1966), **Hyperfiltration Studies (IV) Salt Rejection by Dynamically Formed Hydrous Oxide Membrane**, *Journal of American Chemical Society*, **88**, pp. 5744

NAKAO, S., NOMURA, T., KIMURA, S. and WATANABE, A. (1986), **Formation and Characteristics of Inorganic Dynamic Membranes for Ultrafiltration**, *Journal of Chemical Engineering of Japan*, **19(3)**, pp 221-227

NOMURA, T. and KIMURA, S. (1980), **Properties of Dynamically Formed Membranes**, *Desalination*, **32**, pp. 57-63

NEYTZELL-DE-WILDE, F.G., BUCKLEY, C.A. and CAWDRON, M.P.R. (1988), **Dynamically Formed Hydrous Zirconium (IV) Oxide/Polyacrylic Membranes; Low Pressure Formation, High Pressure Evaluation**, *Desalination*, **70**, pp. 121-136

OHTANI, T., NAKAJIMA, Y. and WATANABE, A. (1991), **Formation of Dynamic UF Membrane with Fine Zr Particles**, *Journal of Membrane Science*, **64**, pp. 273-281

PILLAY, V.L. (1992), **Modelling of Turbulent Cross-Flow Microfiltration of Particulate Suspensions**, Phd Thesis, University of Natal, Durban

ROMERO, C.A. and DAVIS, R.H. (1988), **Global Model of Crossflow Microfiltration Based on Hydrodynamic Particle Diffusion**, *Journal of Membrane Science*, **39**, pp.157-185

RUSHTON, A., HOSSEINI, M. and RUSHTON, ALAN (1979), **Shear Effects in Cake Formation Mechanisms**, *Filtration & Separation*, **Sept/Oct**, pp. 456-458

SCHNEIDER, K. (1982), **The Concentration of Suspensions by Means of Crossflow-Microfiltration**, *Desalination*, **41**, pp. 263-275

SHOU, J.K., COLLINS, D.J., DO, D.M. and SCHARFF, R.P. (1980), **Precoat Filtration of Coal Liquid Feasibility Study of Bottom Ash Precoat**, *Separation Science and Technology*, **15**(3), pp. 201-221

SONG, L. (1998), **Flux Decline in Crossflow Microfiltration and Ultrafiltration: Mechanisms and Modeling of Membrane Fouling**, *Journal of Membrane Science*, **139**, pp.183-200

SWART, A.F (1993), **Considerations in the Selection of the Operating Regimes for Microfiltration**, MScEng Thesis, University of Natal, Durban

TARLETON, E.S. and WAKEMAN, R.J. (1993), **Understanding Flux Decline in Crossflow Microfiltration: Part I – Effects of Particle and Pore Size**, *Trans IChemE*, **71**, pp. 399-410

TARLETON, E.S. and WAKEMAN, R.J. (1994), **Understanding Flux Decline in Crossflow Microfiltration: Part II – Effects of Process Parameters**, *Trans IChemE*, **72**, pp. 431-440

TOWNSEND, R.B., NEYTZELL-DE WILDE, F.G., BUCKLEY, C.A., TURPIE, D.W.F. and STEENKAMP, C. (1992), **The Use of Dynamic Membranes for the Treatment of Effluents Arising from Wool Scouring and Textile Dyeing Effluents**, *Water SA*, **18**, pp 81-86

TREFFRY-GOATLEY, K., BUIJS, K.R., BINDOFF, A.M. and BUCKLEY, C.A. (1987), **The Cross-Flow Microfiltration of Problematic Surface and River Waters to Produce Potable Water**, *Desalination*, **67**, pp. 439-453

TURKSON, A.K., MIKHLIN, J.A. and WEBER, M.E. (1989/90), **Dynamic Membranes. 1. Determination of Optimum Formation Conditions and Electrofiltration of Bovine Serum Albumin with a Rotating Module**, *Separation Science and Technology*, **24**(15), pp. 1261-1291

WAKEMAN, R.J (1994), **Visualisation of Cake Formation in Crossflow Microfiltration**, *Trans IChemE*, 72, pp. 530-540

YANG, C., ZHANG, G., XU, N. and SHI, J. (1998), **Preparation and Application in Oil-Water Separation of ZrO_2/α-Al_2O_3 MF Membrane**, *Journal of Membrane Science*, 142, pp. 235-243

Appendix

RESULTS OF EXPERIMENTAL STUDY

RUN 1		
Artificial Feed Suspension :		
Bulk Concentration	(g/l)	0.05
Superficial Inlet Velocity	(m/s)	1.9
Pressure	(kPa)	200
Turbidity	(NTU)	18
Time from Start-up (minutes)	Permeate Flux ($l/m^2.h$)	Permeate Turbidity (NTU)
Feed Suspension		
5	592	
10	396	
20	309	
30	254	
60	187	
90	164	
120	144	
180	131	
240	122	
300	115	
360	114	

RUN 2		
Precoat Conditions :		
Bulk Concentration	(g/l)	5
Superficial Inlet Velocity	(m/s)	1.9
Pressure	(kPa)	200
Average Particle Size	(μm)	5
Time from Start-up (minutes)	Permeate Flux ($l/m^2.h$)	Permeate Turbidity (NTU)
Precoating Period		
5	1805	
10	1430	
20	1186	
30	1003	
Switchover to Feed Suspension		
5	952	
10	822	
20	661	
30	520	
60	431	
90	374	
120	353	
180	319	
240	306	
300	299	
360	291	

RUN 3		
Precoat Conditions :		
Bulk Concentration	(g/l)	5
Superficial Inlet Velocity	(m/s)	1.0
Pressure	(kPa)	200
Average Particle Size	(μm)	5
Time from Start-up (minutes)	Permeate Flux ($l/m^2.h$)	Permeate Turbidity (NTU)
Precoating Period		
5	1976	
10	1480	
20	1143	
30	1031	
Switchover to Feed Suspension		
5	849	
10	699	
20	566	
30	490	
60	359	
90	322	
120	276	
180	261	
240	253	
300	239	
360	225	

RUN 4		
Precoat Conditions :		
Bulk Concentration	(g/l)	5
Superficial Inlet Velocity	(m/s)	2.5
Pressure	(kPa)	200
Average Particle Size	(μm)	5
Time from Start-up (minutes)	Permeate Flux ($l/m^2.h$)	Permeate Turbidity (NTU)
Precoating Period		
5	2038	
10	1446	
20	1131	
30	1206	
Switchover to Feed Suspension		
5	970	
10	823	
20	646	
30	538	
60	416	
90	368	
120	333	
180	302	
240	296	
300	286	
360	277	

RUN 5		
Precoat Conditions :		
Bulk Concentration	(g/l)	5
Superficial Inlet Velocity	(m/s)	2.5
Pressure	(kPa)	200
Average Particle Size	(μm)	5
Time from Start-up (minutes)	Permeate Flux ($l/m^2.h$)	Permeate Turbidity (NTU)
Precoating Period		
5	2167	
10	1692	
20	1260	
30	1102	
Switchover to Feed Suspension		
5	996	
10	840	
20	637	
30	543	
60	426	
90	383	
120	345	
180	318	
240	310	
300	292	
360	280	

RUN 6		
Precoat Conditions :		
Bulk Concentration	(g/l)	5
Superficial Inlet Velocity	(m/s)	1.0
Pressure	(kPa)	200
Average Particle Size	(μm)	5
Time from Start-up (minutes)	Permeate Flux ($l/m^2.h$)	Permeate Turbidity (NTU)
Precoating Period		
5	2115	
10	1584	
20	1218	
30	1085	
Switchover to Feed Suspension		
5	878	
10	739	
20	599	
30	510	
60	391	
90	330	
120	307	
180	279	
240	273	
300	259	
360	249	

RUN 7		
Precoat Conditions :		
Bulk Concentration	(g/l)	5
Superficial Inlet Velocity	(m/s)	1.9
Pressure	(kPa)	100
Average Particle Size	(μm)	5
Time from Start-up (minutes)	Permeate Flux ($l/m^2.h$)	Permeate Turbidity (NTU)
Precoating Period		
5	1255	
10	1052	
20	933	
30	877	
Switchover to Feed Suspension		
5	1213	
10	828	
20	591	
30	501	
60	398	
90	349	
120	322	
180	300	
240	276	
300	271	
360	264	

RUN 8		
Precoat Conditions :		
Bulk Concentration	(g/l)	5
Superficial Inlet Velocity	(m/s)	1.9
Pressure	(kPa)	300
Average Particle Size	(μm)	5
Time from Start-up (minutes)	Permeate Flux ($l/m^2.h$)	Permeate Turbidity (NTU)
Precoating Period		
5	2688	
10	2174	
20	1626	
30	1494	
Switchover to Feed Suspension		
5	788	
10	683	
20	595	
30	516	
60	406	
90	354	
120	325	
180	292	
240	276	
300	272	
360	263	

RUN 9		
Precoat Conditions :		
Bulk Concentration	(g/l)	5
Superficial Inlet Velocity	(m/s)	1.9
Pressure	(kPa)	200
Average Particle Size	(μm)	5
Time from Start-up (minutes)	Permeate Flux ($l/m^2.h$)	Permeate Turbidity (NTU)
Precoating Period		
5	1966	
10	1490	
20	1208	
30	1099	
Switchover to Feed Suspension		
5	980	
10	851	
20	688	
30	593	
60	456	
90	374	
120	356	
180	331	
240	307	
300	296	
360	292	

RUN 10		
Precoat Conditions :		
Bulk Concentration	(g/l)	5
Superficial Inlet Velocity	(m/s)	1.9
Pressure	(kPa)	100
Average Particle Size	(μm)	5
Time from Start-up (minutes)	Permeate Flux ($l/m^2.h$)	Permeate Turbidity (NTU)
Precoating Period		
5	1209	
10	1042	
20	932	
30	863	
Switchover to Feed Suspension		
5	1125	
10	823	
20	624	
30	517	
60	416	
90	361	
120	333	
180	315	
240	306	
300	285	
360	276	

RUN 11		
Precoat Conditions :		
Bulk Concentration	(g/l)	2
Superficial Inlet Velocity	(m/s)	1.9
Pressure	(kPa)	200
Average Particle Size	(μm)	5
Time from Start-up (minutes)	Permeate Flux ($l/m^2.h$)	Permeate Turbidity (NTU)
Precoating Period		
5	3101	
10	2206	
20	1779	
30	1527	
Switchover to Feed Suspension		
5	1157	
10	839	
20	607	
30	512	
60	394	
90	327	
120	314	
180	284	
240	267	
300	258	
360	250	

RUN 12		
Precoat Conditions :		
Bulk Concentration	(g/l)	20
Superficial Inlet Velocity	(m/s)	1.9
Pressure	(kPa)	200
Average Particle Size	(μm)	5
Time from Start-up (minutes)	Permeate Flux ($l/m^2.h$)	Permeate Turbidity (NTU)
Precoating Period		
5	1149	
10	965	
20	914	
30	899	
Switchover to Feed Suspension		
5	809	
10	725	
20	662	
30	599	
60	542	
90	504	
120	485	
180	465	
240	449	
300	440	
360	435	

RUN 13		
Precoat Conditions :		
Bulk Concentration	(g/l)	5
Superficial Inlet Velocity	(m/s)	1.9
Pressure	(kPa)	150
Average Particle Size	(μm)	5
Time from Start-up (minutes)	Permeate Flux ($l/m^2.h$)	Permeate Turbidity (NTU)
Precoating Period		
5	1968	
10	1502	
20	1278	
30	1202	
Switchover to Feed Suspension		
5	1218	2.98
10	918	1.78
20	641	1.42
30	553	0.50
60	429	0.33
90	381	0.25
120	350	0.20
180	312	0.12
240	306	0.15
300	302	0.12
360	298	0.11

RUN 14		
Precoat Conditions :		
Bulk Concentration	(g/l)	5
Superficial Inlet Velocity	(m/s)	1.9
Pressure	(kPa)	250
Average Particle Size	(μm)	5
Time from Start-up (minutes)	Permeate Flux ($l/m^2.h$)	Permeate Turbidity (NTU)
Precoating Period		
5	2467	
10	2040	
20	1701	
30	1584	
Switchover to Feed Suspension		
5	980	3.24
10	840	1.67
20	653	0.43
30	562	0.24
60	419	0.15
90	376	0.12
120	348	0.10
180	330	-
240	304	0.18
300	287	0.12
360	281	0.12

RUN 15		
Precoat Conditions :		
Bulk Concentration	(g/l)	5
Superficial Inlet Velocity	(m/s)	3.0
Pressure	(kPa)	200
Average Particle Size	(μm)	5
Time from Start-up (minutes)	Permeate Flux ($l/m^2.h$)	Permeate Turbidity (NTU)
Precoating Period		
5	2783	
10	2251	
20	1881	
30	1763	
Switchover to Feed Suspension		
5	1061	4.21
10	797	2.00
20	570	1.02
30	488	0.66
60	380	0.23
90	327	0.18
120	301	0.15
180	269	0.11
240	258	0.14
300	258	0.10
360	249	0.13

RUN 16		
Precoat Conditions :		
Bulk Concentration	(g/l)	5
Superficial Inlet Velocity	(m/s)	1.5
Pressure	(kPa)	200
Average Particle Size	(μm)	5
Time from Start-up (minutes)	Permeate Flux ($l/m^2.h$)	Permeate Turbidity (NTU)
Precoating Period		
5	2211	
10	1694	
20	1371	
30	1249	
Switchover to Feed Suspension		
5	907	2.14
10	810	1.16
20	621	0.65
30	521	0.58
60	392	0.22
90	339	0.15
120	322	0.18
180	298	0.16
240	280	0.15
300	272	0.13
360	267	0.09

RUN 17		
Precoat Conditions :		
Bulk Concentration	(g/l)	10
Superficial Inlet Velocity	(m/s)	1.9
Pressure	(kPa)	200
Average Particle Size	(μm)	5
Time from Start-up (minutes)	Permeate Flux ($l/m^2.h$)	Permeate Turbidity (NTU)
Precoating Period		
5	1764	
10	1439	
20	1206	
30	1102	
Switchover to Feed Suspension		
5	982	4.66
10	830	4.45
20	647	1.25
30	534	0.99
60	432	0.41
90	376	0.33
120	354	0.22
180	337	0.18
240	322	0.15
300	298	0.17
360	294	0.16

RUN 18		
Precoat Conditions :		
Bulk Concentration	(g/l)	5
Superficial Inlet Velocity	(m/s)	1.9
Pressure	(kPa)	200
Average Particle Size	(μm)	5
Time from Start-up (minutes)	Permeate Flux ($l/m^2.h$)	Permeate Turbidity (NTU)
Precoating Period		
5	2145	147.0
10	1690	164.0
20	1435	90.5
30	1283	44.1
60	1130	28.2
Switchover to Feed Suspension		
5	922	4.11
10	764	1.89
20	566	0.76
30	470	0.45
60	348	0.32
90	311	0.20
120	278	0.20
180	255	0.16
240	235	0.13
300	230	0.12
360	215	0.10

RUN 19		
Precoat Conditions :		
Bulk Concentration	(g/l)	5
Superficial Inlet Velocity	(m/s)	1.9
Pressure	(kPa)	200
Average Particle Size	(μm)	5
Time from Start-up (minutes)	Permeate Flux ($l/m^2.h$)	Permeate Turbidity (NTU)
Precoating Period		
5	2088	64.1
10	1701	31.7
20	1382	15.5
Switchover to Feed Suspension		
5	1063	2.00
10	839	1.45
20	601	0.79
30	519	0.80
60	394	0.22
90	339	0.15
120	308	
180	287	0.12
240	268	0.13
300	265	
360	256	

RUN 20		
Precoat Conditions :		
Bulk Concentration	(g/l)	5
Superficial Inlet Velocity	(m/s)	1.9
Pressure	(kPa)	200
Average Particle Size	(μm)	5
Time from Start-up (minutes)	Permeate Flux ($l/m^2.h$)	Permeate Turbidity (NTU)
Precoating Period		
5	1974	14.6
10	1640	10.6
20	1393	2.87
30	1273	0.25
60	1228	0.12
Switchover to Feed Suspension		
5	953	0.18
10	766	1.02
20	556	0.87
30	462	0.33
60	375	0.18
90	316	0.15
120	290	0.16
180	267	0.13
240	249	0.12
300	236	0.12
360	222	0.11

RUN 21		
Precoat Conditions :		
Bulk Concentration	(g/l)	5
Superficial Inlet Velocity	(m/s)	1.9
Pressure	(kPa)	200
Average Particle Size	(μm)	5
Time from Start-up (minutes)	Permeate Flux ($l/m^2.h$)	Permeate Turbidity (NTU)
Precoating Period		
5	2186	137
10	1748	145
20	1457	222
Switchover to Feed Suspension		
5	1108	6.16
10	859	3.44
20	617	2.92
30	533	1.47
60	405	0.43
90	363	0.71
120	306	0.21
180	285	0.19
240	275	0.20
300	266	0.18
360	264	0.25

RUN 22		
Precoat Conditions :		
Bulk Concentration	(g/l)	50
Superficial Inlet Velocity	(m/s)	1.9
Pressure	(kPa)	200
Average Particle Size	(μm)	5
Time from Start-up (minutes)	Permeate Flux ($l/m^2.h$)	Permeate Turbidity (NTU)
Precoating Period		
5	905	437
10	842	408
20	771	325
30	725	319
Switchover to Feed Suspension		
5	712	7.05
10	696	8.75
20	670	10.2
30	640	6.70
60	596	3.33
90	580	4.89
120	558	4.45
180	546	1.90
240	542	0.87
300	542	0.62
360	540	0.76

RUN 23		
Precoat Conditions :		
Bulk Concentration	(g/l)	5
Superficial Inlet Velocity	(m/s)	1.9
Pressure	(kPa)	200
Average Particle Size	(μm)	5
Time from Start-up (minutes)	Permeate Flux ($l/m^2.h$)	Permeate Turbidity (NTU)
Precoating Period		
5	2174	173
10	1687	116
20	1319	57.5
25	1285	43.1
Switchover to Feed Suspension		
5	1080	2.88
10	857	3.11
20	643	2.69
30	546	1.77
60	403	0.79
90	359	0.28
120	345	0.27
180	306	0.24
240	294	0.59
300	288	0.73
360	270	0.30

RUN 24		
Precoat Conditions :		
Bulk Concentration	(g/l)	5
Superficial Inlet Velocity	(m/s)	1.9
Pressure	(kPa)	200
Average Particle Size	(μm)	5
Time from Start-up (minutes)	Permeate Flux ($l/m^2.h$)	Permeate Turbidity (NTU)
Precoating Period		
5	2102	34.5
10	1553	30.5
15	1405	21.3
Switchover to Feed Suspension		
5	1130	0.92
10	849	0.76
20	647	0.49
30	556	0.36
60	486	0.26
90	435	0.23
120	298	0.22
180	385	0.15
240	376	0.15
300	373	0.14
360	372	0.09

RUN 25		
Precoat Conditions :		
Bulk Concentration	(g/l)	5
Superficial Inlet Velocity	(m/s)	1.9
Pressure	(kPa)	200
Average Particle Size	(μm)	5
Time from Start-up (minutes)	Permeate Flux ($l/m^2.h$)	Permeate Turbidity (NTU)
Precoating Period		
5	2108	222
10	1637	204
20	1371	166
25	1247	90.5
Switchover to Feed Suspension		
5	1002	5.58
10	758	3.53
20	534	2.32
30	468	1.78
60	346	0.51
90	306	0.32
120	291	0.27
180	259	0.25
240	244	0.22
300	238	0.22
360	229	0.26

RUN 26		
Precoat Conditions :		
Bulk Concentration	(g/l)	5
Superficial Inlet Velocity	(m/s)	1.9
Pressure	(kPa)	200
Average Particle Size	(μm)	5
Time from Start-up (minutes)	Permeate Flux ($l/m^2.h$)	Permeate Turbidity (NTU)
Precoating Period		
5	2059	176
10	1639	145
15	1458	142
Switchover to Feed Suspension		
5	1083	6.04
10	779	4.20
20	549	2.11
30	472	2.10
60	358	0.45
90	319	0.31
120	296	0.25
180	269	0.14
240	256	0.14
300	253	0.12
360	249	0.11

RUN 27		
Precoat Conditions :		
Bulk Concentration	(g/l)	5
Superficial Inlet Velocity	(m/s)	1.9
Pressure	(kPa)	200
Average Particle Size	(μm)	2
Time from Start-up (minutes)	Permeate Flux ($l/m^2.h$)	Permeate Turbidity (NTU)
Precoating Period		
5	1692	
10	1266	
20	1002	
30	900	
Switchover to Feed Suspension		
5	781	
10	698	
20	594	
30	508	
60	413	
90	369	
120	347	
180	318	
240	304	
300	289	
360	282	

RUN 28		
Precoat Conditions :		
Bulk Concentration	(g/l)	5
Superficial Inlet Velocity	(m/s)	1.9
Pressure	(kPa)	200
Average Particle Size	(μm)	10
Time from Start-up (minutes)	Permeate Flux ($l/m^2.h$)	Permeate Turbidity (NTU)
Precoating Period		
5	2143	
10	1614	
20	1387	
30	1261	
Switchover to Feed Suspension		
5	1013	
10	794	
20	583	
30	497	
60	391	
90	367	
120	330	
180	302	
240	275	
300	267	
360	263	

RUN 29		
Precoat Conditions :		
Bulk Concentration	(g/l)	5
Superficial Inlet Velocity	(m/s)	1.9
Pressure	(kPa)	200
Average Particle Size	(μm)	40
Time from Start-up (minutes)	Permeate Flux ($l/m^2.h$)	Permeate Turbidity (NTU)
Precoating Period		
5	3223	
10	2480	
20	1970	
30	1795	
Switchover to Feed Suspension		
5	1192	
10	850	
20	632	
30	520	
60	422	
90	378	
120	355	
180	338	
240	310	
300	299	
360	296	

RUN 30		
Precoat Conditions :		
Bulk Concentration	(g/l)	5
Superficial Inlet Velocity	(m/s)	1.9
Pressure	(kPa)	200
Average Particle Size	(μm)	10
Time from Start-up (minutes)	Permeate Flux ($l/m^2.h$)	Permeate Turbidity (NTU)
Precoating Period		
5	2162	
10	1712	
20	1389	
30	1302	
Switchover to Feed Suspension		
5	953	
10	779	
20	609	
30	516	
60	406	
90	377	
120	338	
180	315	
240	296	
300	288	
360	270	

RUN 31		
Precoat Conditions :		
Bulk Concentration	(g/l)	5
Superficial Inlet Velocity	(m/s)	1.9
Pressure	(kPa)	200
Average Particle Size	(μm)	5
Time from Start-up (minutes)	Permeate Flux ($l/m^2.h$)	Permeate Turbidity (NTU)
Precoating Period		
5	1970	144.0
10	1536	98.0
20	1286	66.8
30	1189	
Switchover to Feed Suspension		
5	1013	1.61
10	791	2.07
20	610	0.99
30	534	0.88
60	413	0.45
90	367	0.20
120	332	0.18
180	314	0.24
240	304	0.18
300	288	0.10
360	279	0.91

RUN 32		
Precoat Conditions :		
Bulk Concentration	(g/l)	5
Superficial Inlet Velocity	(m/s)	1.9
Pressure	(kPa)	200
Average Particle Size	(μm)	5
Time from Start-up (minutes)	Permeate Flux ($l/m^2.h$)	Permeate Turbidity (NTU)
Precoating Period		
5	1752	
10	1386	
20	1130	
30	1044	
Switchover to Feed Suspension		
5	961	
10	823	
20	617	
30	514	
60	391	
90	357	
120	313	
180	303	
240	289	
300	285	
360	274	

RUN 33		
Precoat Conditions :		
Bulk Concentration	(g/l)	10
Superficial Inlet Velocity	(m/s)	1.9
Pressure	(kPa)	200
Average Particle Size	(μm)	5
Time from Start-up (minutes)	Permeate Flux ($l/m^2.h$)	Permeate Turbidity (NTU)
Precoating Period		
5	1766	
10	1374	
20	1105	
30	980	
Switchover to Feed Suspension		
5	868	
10	763	
20	605	
30	527	
60	418	
90	391	
120	353	
180	322	
240	312	
300	306	
360	298	

RUN 34		
Precoat Conditions :		
Bulk Concentration	(g/l)	20
Superficial Inlet Velocity	(m/s)	1.9
Pressure	(kPa)	200
Average Particle Size	(μm)	5
Time from Start-up (minutes)	Permeate Flux ($l/m^2.h$)	Permeate Turbidity (NTU)
Precoating Period		
5	1386	
10	1245	
20	977	
30	841	
Switchover to Feed Suspension		
5	776	
10	720	
20	636	
30	575	
60	482	
90	440	
120	432	
180	414	
240	391	
300	392	
360	390	

RUN 35		
Precoat Conditions :		
Bulk Concentration	(g/l)	5
Superficial Inlet Velocity	(m/s)	1.9
Pressure	(kPa)	200
Average Particle Size	(μm)	2
Time from Start-up (minutes)	Permeate Flux ($l/m^2.h$)	Permeate Turbidity (NTU)
Precoating Period		
5	1415	
10	1037	
20	842	
30	807	
Switchover to Feed Suspension		
5	750	
10	696	
20	602	
30	527	
60	419	
90	372	
120	363	
180	322	
240	314	
300	307	
360	300	

RUN 36		
Precoat Conditions :		
Bulk Concentration	(g/l)	5
Superficial Inlet Velocity	(m/s)	1.9
Pressure	(kPa)	200
Average Particle Size	(μm)	40
Time from Start-up (minutes)	Permeate Flux ($l/m^2.h$)	Permeate Turbidity (NTU)
Precoating Period		
5	3451	
10	2499	
20	2003	
30	1822	
Switchover to Feed Suspension		
5	1007	
10	710	
20	517	
30	427	
60	343	
90	296	
120	265	
180	248	
240	232	
300	228	
360	222	

RUN 37		
Feed Suspension Conditions :		
Bulk Concentration	(g/l)	0.05
Superficial Inlet Velocity	(m/s)	1.9
Pressure	(kPa)	200
Time from Start-up (minutes)	Permeate Flux ($l/m^2.h$)	Permeate Turbidity (NTU)
Feed Suspension		
5	680	2.07
10	469	1.40
20	379	0.87
30	308	0.68
60	244	0.78
90	213	-
120	200	-
180	182	-
240	172	-
300	161	0.69
360	148	0.65

RUN 38		
Precoat Conditions :		
Bulk Concentration	(g/l)	5
Superficial Inlet Velocity	(m/s)	1.9
Pressure	(kPa)	200
Average Particle Size	(μm)	5
Time from Start-up (minutes)	Permeate Flux ($l/m^2.h$)	Permeate Turbidity (NTU)
Precoating Period		
5	1930	2.86
10	1438	0.86
20	1191	0.34
30	1092	0.16
40	1024	0.14
Switchover to Feed Suspension		
5	913	0.86
10	768	0.96
20	589	0.29
30	476	0.14
60	367	0.62
90	321	0.10
120	293	0.09
180	280	0.07
240	265	0.15
300	251	0.10
360	241	0.09

RUN 39		
Precoat Conditions :		
Bulk Concentration	(g/l)	5
Superficial Inlet Velocity	(m/s)	1.9
Pressure	(kPa)	200
Average Particle Size	(μm)	5
Time from Start-up (minutes)	Permeate Flux ($l/m^2.h$)	Permeate Turbidity (NTU)
Precoating Period		
5	2349	1060
10	1976	884
20	1481	610
30	1317	419
Switchover to Feed Suspension		
5	1011	25.6
10	872	15.2
20	610	7.19
30	528	5.63
60	413	1.96
90	359	1.81
120	337	1.47
180	307	1.93
240	296	1.33
300	297	1.71
360	285	0.81

RUN 40		
Precoat Conditions :		
Bulk Concentration	(g/l)	5
Superficial Inlet Velocity	(m/s)	1.9
Pressure	(kPa)	200
Average Particle Size	(μm)	5
Time from Start-up (minutes)	Permeate Flux ($l/m^2.h$)	Permeate Turbidity (NTU)
Precoating Period		
5	2700	
10	1963	
20	1449	
30	1239	
Switchover to Feed Suspension		
5	1076	
10	909	
20	702	
30	597	
60	450	
90	399	
120	360	
180	337	
240	319	
300	307	
360	294	

RUN 41		
Precoat Conditions :		
Bulk Concentration	(g/l)	5
Superficial Inlet Velocity	(m/s)	1.9
Pressure	(kPa)	300
Average Particle Size	(μm)	5
Time from Start-up (minutes)	Permeate Flux ($l/m^2.h$)	Permeate Turbidity (NTU)
Precoating Period		
5	2942	1386
10	2538	987
20	1632	533
30	1375	392
Switchover to Feed Suspension		
5	767	34.0
10	700	9.36
20	640	6.10
30	576	4.96
60	465	4.01
90	406	3.14
120	359	3.52
180	326	2.31
240	315	1.87
300	305	1.21
360	300	1.10

RUN 42		
Precoat Conditions :		
Bulk Concentration	(g/l)	5
Superficial Inlet Velocity	(m/s)	3.0
Pressure	(kPa)	200
Average Particle Size	(μm)	5
Time from Start-up (minutes)	Permeate Flux ($l/m^2.h$)	Permeate Turbidity (NTU)
Precoating Period		
5	1502	375
10	1336	197
20	1285	101
30	1237	59
Switchover to Feed Suspension		
5	936	5.03
10	805	3.15
20	615	2.96
30	530	2.75
60	421	1.37
90	391	1.23
120	376	1.81
180	341	1.77
240	331	2.13
300	320	2.31
360	311	1.96

RUN 43		
Precoat Conditions :		
Bulk Concentration	(g/l)	5
Superficial Inlet Velocity	(m/s)	1.9
Pressure	(kPa)	200
Average Particle Size	(μm)	5
Time from Start-up (minutes)	Permeate Flux ($l/m^2.h$)	Permeate Turbidity (NTU)
Precoating Period		
5	1800	
10	1346	
20	1159	
30	1067	
Switchover to Feed Suspension		
5	914	
10	807	
20	634	
30	535	
60	415	
90	363	
120	333	
180	309	
240	308	
300	297	
360	291	